UNIVERSITÀ DEGLI STUDI DI PADOVA

DIPARTIMENTO DI SCIENZE DEL FARMACO

CORSO DI LAUREA MAGISTRALE IN
PHARMACEUTICAL BIOTECHNOLOGIES
BIOTECNOLOGIE FARMACEUTICHE

TESI DI LAUREA

IMMUNOLOGICAL ORCHESTRATION OF LIVER FIBROSIS AND REGENERATION IN MALE AND FEMALE MICE

Relatore: Chiar.ma Prof.ssa Sara De Martin

Laureanda: Giulia Danieli

Matricola: 1239219

ANNO ACCADEMICO 2021-2022

TABLE OF CONTENTS

RIASSUNTO

Introduzione e scopo. La fibrosi epatica è una patologia del fegato di origine infiammatoria causata dalla iperproduzione e deposizione di collagene e tessuto connettivo nel parenchima epatico. Questa deposizione è dovuta ad un danno cronico conseguente a patologie del fegato di diversa eziologia, per le quali si osservano incidenza e decorso differenti nel genere maschile e femminile.

Le cellule epatiche stellate (hepatic stellate cells, HSCs) hanno un ruolo chiave nella fibrogenesi, in quanto, in seguito alla loro attivazione da parte di citochine e chemochine pro-infiammatorie prodotte da epatociti danneggiati e cellule di Kupffer, esse transdifferenziano in miofibroblasti, dotati di attività proinfiammatoria e fibrogenica.

Durante le prime fasi della fibrogenesi, avviene anche il recultamento ed attivazione delle cellule immunitarie, tra cui neutrofili e macrofagi derivanti da monociti (Momφs), che possiedono a loro volta un'azione proinfiammatoria e profibrotica. Infiltrandosi nel parenchima epatico, essi promuovono la deposizione di matrice extracellulare, l'ulteriore attivazione delle HSC e dunque la progressione della fibrosi.

Il fegato può mettere in atto meccanismi di riparazione tissutale, dopo la rimozione della fonte del danno. Durante la rigenerazione, le HSC attivate vanno incontro ad apoptosi e gli epatociti danneggiati vengono sostituiti da cellule sane. I macrofagi infiltrati, che nelle fasi di induzione del danno epatico iperesprimono l'antigene Ly6C ($Ly6C^{high}$) cambiano il fenotipo in $Ly6C^{low}$, promuovendo l'apoptosi delle HSC e contribuendo alla rigenerazione. Inoltre, in questa fase si riattivano le metalloproteinasi, che degradano la matrice extracellulare.

L'obiettivo di questo studio in vivo è stata la valutazione delle differenze di genere nei processi di fibrogenesi e rigenerazione del danno epatico, con particolare attenzione alla valutazione del fenotipo dell'infiltrato immunitario, in un modello murino di fibrosi epatica ottenuto mediante la somministrazione di dosi crescenti dell'agente epatotossico tetracloruro di carbonio (CCl_4) a topi maschi e femmina.

Materiali e metodi. Sono stati utilizzati 60 topi (30 maschi e 30 femmine Balb/cJ), randomizzati e divisi in un gruppo di controllo (15 maschi e 15 femmine) e uno trattato (15 maschi e 15 femmine). Essi sono stati sottoposti a iniezioni intraperitoneali di veicolo (olio di semi) o di CCl_4 due volte alla settimana. Cinque animali per genere sono stati sacrificati ad ogni timepoint (6 e 12 settimane di trattamento, seguite da 8 di recovery) A

seguito del sacrificio, il fegato è stato rimosso e sottoposto ad esame istologico con la colorazione tricromica di Masson per evidenziare i setti fibrotici. Le HSC attivate sono state individuate mediante valutazione di alpha-SMA. Inoltre, sono stati valutati i livelli di espressione di metalloproteinasi (MMPs) e gli inibitori tissutali delle metalloproteinasi (TIMPs) attraverso l'immunoistochimica. Il numero di cellule immunitarie presenti durante il processo fibrotico e di rigenerazione, come neutrofili, linfociti ed NK, cellule di Kupffer e macrofagi infiltrati che esprimono l'antigene Ly6C sono stati valutati mediante citofluorimetria eseguita sul tessuto epatico appena asportato. Infine, è stata valutata l'espressione di alcuni geni coinvolti nella fibrogenesi (Col1a1, TNFalpha, TGFbeta, CCL2, PDGFA, VEGFA) mediante qRT-PCR.

Risultati e conclusioni. Il protocollo utilizzato, che prevede dosi crescenti di CCl_4, ha determinato lo sviluppo di fibrosi nei topi di entrambi i generi nelle dodici settimane di trattamento. Alla sospensione, gli animali hanno dimostrato una regressione della fibrosi e una diminuzione dei processi infiammatori prima attivati.

I topi maschi hanno sviluppato fibrosi più velocemente delle femmine, come dimostrato dall'analisi istologica, dall'espressione genica di Col1a1, dalla quantificazione di αSMA, dall'aumento degli inibitori delle metalloproteinasi, dall'analisi istologica, dall'espressione genica delle citochine proinfiammatorie TGFbeta e dal numero di macrofagi proinfiammatori e neutrofili reclutati, tutti più elevati nei topi maschi rispetto alle femmine dopo 6 settimane di trattamento. Invece, nei topi femmina si è osservato un danno più graduale. Infatti, dopo dodici settimane, esse mostrano una percentuale maggiore di collagene, un aumentato livello di inibitori delle metalloproteinasi e diminuita espressione delle metalloproteinasi. Anche lo stato infiammatorio è peggiorato notevolmente rispetto alle 6 settimane, come dimostrato dall'incremento del reclutamento dei macrofagi. Dopo il periodo di washout, è stata evidenziata una migliore capacità di rigenerazione delle femmine che, rispetto ai maschi, hanno una minore deposizione di collagene, una riduzione dell'attivazione delle HSC e un significativo decremento degli inibitori delle metalloproteasi al termine del periodo di washout. In conclusione, il nostro studio dimostra che esistono delle differenze di genere nei processi di fibrogenesi e rigenerazione del fegato, che correlano con il fenotipo delle cellule immunitarie infiltranti il parenchima epatico.

ABSTRACT

Introduction: Liver fibrosis is a wound-healing response against chronic insult that leads to an alteration of the homeostasis within the hepatic parenchyma. The main contributors to this disequilibrium are the inflammatory processes that activate Hepatic Stellate Cells, the principal initiators of fibrogenesis. Fibrogenesis leads to advanced stages of liver fibrosis that can either result in cirrhosis, an irreversible condition of liver damage or reverse when the fibrogenic insult is removed. Different studies underline sex-dimorphism in the development and progression of several liver diseases characterized by fibrogenesis, but also in immune reactogenicity.

Aim: This work aims to investigate gender-related differences between male and female mice during liver fibrosis and regeneration, focusing on the regulation of selected immune cells.

Materials and methods: To induce liver fibrosis increasing doses of CCl_4 (from 0.17 to 0.72 uL/g body weight) have been intraperitoneally injected into Balb/C mice for 12 weeks, followed by an 8-week washout period to allow liver regeneration. At sacrifice, fibrosis was assessed by liver histology by Masson's trichrome staining and by measuring the activation of Hepatic Stellate Cells (HSC). Gene expression of pro-inflammatory cytokines was evaluated by qRT-PCR. Flow cytometry experiments were performed on fresh liver tissues to calculate the amount of recruited Monocytes-derived Macrophages (MoMFs), Neutrophils, and Kupffer cells.

Results: The obtained results highlighted that this new model of increasing doses of CCl_4 led to the development of liver damage without adaptive responses of the liver to the injury. In addition, it has been observed that gender influences the recruitment of pro-inflammatory immune cells and the activation of Hepatic Stellate Cells. In particular, the damage occurs more rapidly in males than females, while females recovered better than males from liver damage. This study underlines a sex-related difference during the fibrogenesis and regeneration processes, suggesting the need for further investigations into the mechanisms and role of immune cells with particular attention to the gender difference.

INTRODUCTION

1.1 Human Liver

The liver is the largest organ in the body.[1] It is a brown dome-shaped organ with a smooth surface. [2] The liver weight is about 1500 g in an adult and it is located on the right upper side of the abdominal cavity. [3] It maintains its position thanks to caval ligamentous attachments that are in continuity to Glisson's capsule, an external fibrous layer that envelops liver lobules. [1]

The liver is vascularized by a dual blood supply. The 25% is derived from the hepatic artery which supplies oxygenated blood to the liver, and 75% is due to portal veins arriving from the spleen and intestine. [1] Furthermore, it has two lymphatic networks: superficial and deep. Respectively, the first one is positioned on the Glisson space, while the second one produces the main drainage of lymph deep in the liver**.** [1]

1.1.1 Liver Structure

The liver has two main lobes, called respectively: right and left lobes. The right lobe is the largest one and can be ulteriorly subdivided into caudate and quadrate lobes; while the left lobe is the smallest. [2] From a morphological point of view, the right and the left lobes are separated by the falciform ligament. [1]

Other important ligaments are the gastropathy ligament and the lesser omentum that connect the stomach to the liver. [1] Hepatoduodenal ligament and porta hepatis link duodenum and portal structures to liver. The foramen of Winslow or epiploic foramen represents a connection between the lesser sac and abdominal cavity. [1]

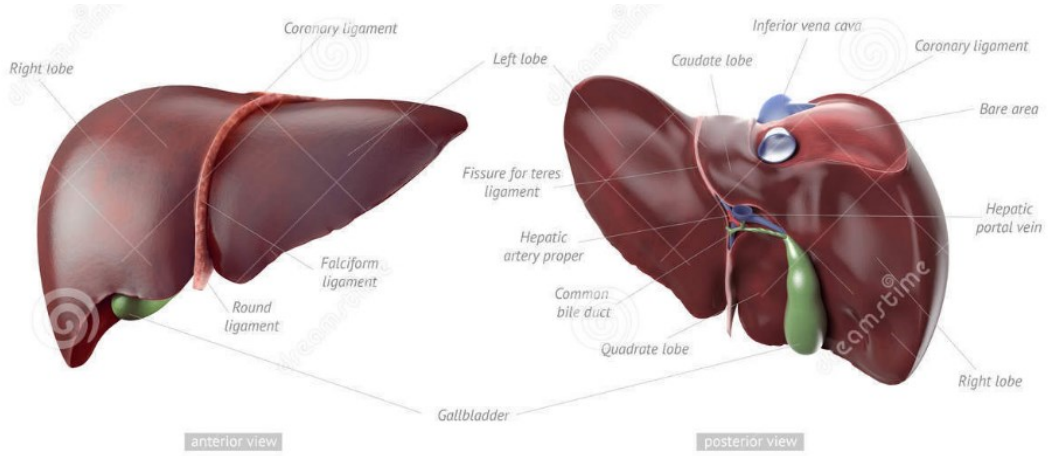

Figure 1 Human liver structure: anterior and posterior point of view.

The liver is divided into eight segments. [4] The left lobe is divided into segment II (anterior left lobe or left lateral segment), III (posterior left lobe or the topographic left lobe), and segment IV (medial segment). [4] The right lobe is composed of segments V and VIII, the anterior segments, and segments VI and VII, the posterior segments. In the end, Segment I, the caudate lobe, is located posteriorly. [4]

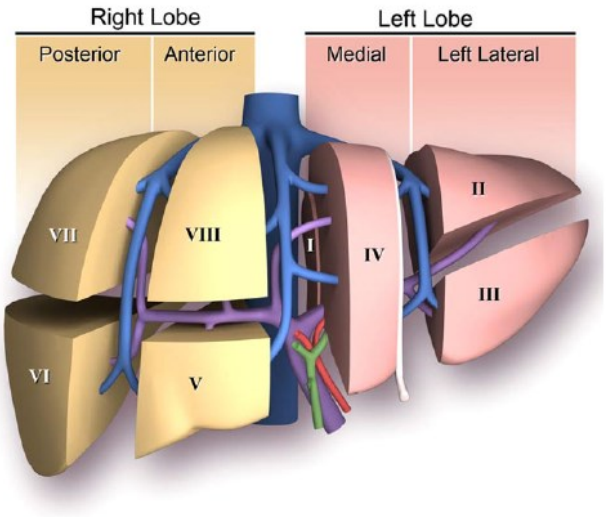

Figure 2 Schematic representation of the liver divided by segments

The hepatic lobule corresponds to the basic functional unit of the liver. [2] The lobule is formed by chords of hepatocytes organized in a hexagonal shape around the central vein. In which vertices are composed of portal triads (association of hepatic artery, portal vein, and bile ducts). [4] Sinusoids run from the central vein to the portal one. [2]

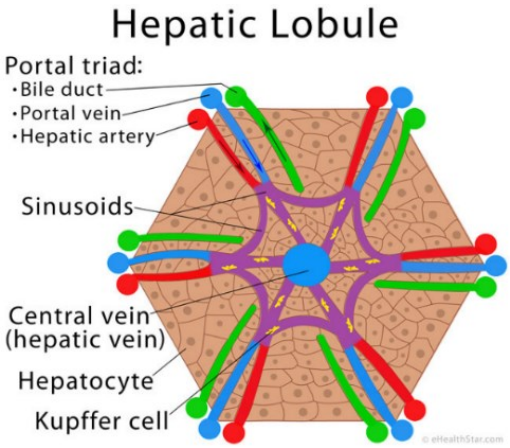

Figure 3 Hepatic lobule structure, with a hexagonal shape. In the middle, there is a central vein. The vertices are composed of bile ducts, portal veins, and hepatic arteries.

The hepatic acinus is the functional unit of the liver. [5] Its shape is like a triangle in which vertices are central veins and portal triads. [6] Based on the perfusion with blood, it can be subdivided into three zones concerning the distance from the arterial blood: [5] [6] *(Figure 4).*

- Zone 1 (or periportal zone): hepatocytes present in this area are in closest proximity to the portal areas. These hepatocytes are metabolically active and receive the maximum oxygen content. They are the first ones to get exposed to toxic substances carried by the portal vein from the gastrointestinal tract. [5] [6]
- Zone 2 (or midzonal): hepatocytes are interspersed between both zones 1 and 3. These cells have considerable regenerative potential. [5] [6]
- Zone 3 (or centrilobular): hepatocytes present here are in the peripheral region of the acinus near the central vein and receive oxygen and nutrient-depleted blood. [5] [6]

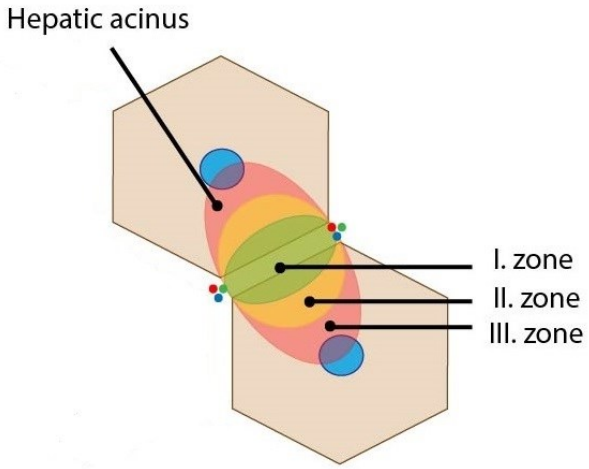

Figure 4 Schematic representation of a hepatic acinus.

1.1.2 Liver functions

The liver is both an endocrine and an exocrine gland. This organ has many functions:

- Produces and secretes bile by also the breakdown of old blood cells.
- Filters blood and secretes substances into the bloodstream.
- Detoxifies and converts drugs and toxic substances into useful substances.
- Stores vitamins, minerals, glycogen, and blood cells.
- Processes hormones, fats, and cholesterol.
- Produces urea.
- Secretes plasma proteins that aid in blood clotting. [7]

1.1.3 Liver cells

Liver cells can be subdivided into two different categories:

1. Parenchymal Cells, which are responsible for the structure of an organism. They are hepatocytes and account for around 60% of the liver's structure. [7]
2. Non-parenchymal cells, which include other types of functional cells. These cells include the Kupffer cells, Endothelial cells, and Hepatic Stellate cells. [7]

Hepatocytes are the primary epithelial cell population of the liver. [1] They are polygonal shaped and polarized and can be either mononucleated or binucleated. [5] Normally, they

are located facing sinusoids with microvilli for better absorption from the plasma or facing other hepatocytes exposed to high concentrations of bile salts for bile formation. They are central to most liver functions including metabolic, secretory, and endocrine functions. They are enriched with dedicated organelles for metabolism functions like mitochondria, peroxisomes, Golgi complexes, and endoplasmic reticulum. [5]

Sinusoidal lining contains different non-parenchymal cell populations such as Kupffer Cells (KC), Sinusoidal Endothelial Cells (SEC), and Hepatic Stellate Cells (HSC). They have a role in liver homeostasis and also in the pathogenesis of liver diseases. [8]

Kupffer cells (KC) are resident macrophages present in the liver. [9] They are irregularly shaped cells with a diameter between 10-13 μm. They are localized in the cavity of liver sinusoids and correspond to 30% of hepatic non-parenchymal cells. Specifically, they are present mainly in the lobule (43%), but also the midzonal (28%) and central area (29%). [8] They can be differentiated and polarized into several subsets based on different markers or functions due to the microenvironment action, for example, M1 phenotype (pro-inflammatory) or M2 phenotype (alternative). Their function is to phagocyte pathogens from blood circulation, contributing to both systemic and hepatic immune responses and acting as the first line of defense from pathogens present in the gastrointestinal tract. [5] Moreover, they are responsible for the production of many cytokines such as TNF alpha, and IL-1, and they are also the major productor of MMP9 in liver fibrosis resolution. [9]

Sinusoidal endothelial cells are unique endothelial cells with an elongated shape that form fenestrated sieve plates at sinusoidal lumens. They are present at the interface of blood cells, HSCs, and hepatocytes. They are responsible for the maintenance of the quiescent state in HSC, for the prevention of intrahepatic vasoconstrictor and fibrosis development. [5]

Hepatic stellate cells (HSC) are a dynamic population present in the liver. They compose about 5-8% of total non-parenchymal cells. The structure is spindle-shaped with an oval or elongated nucleus. [5] Normally, they are present in the subendothelial space between hepatic plates and the antiluminal face of endothelial cells. Their main function is to store and transport retinoids (vitamin A) under the shape of retinyl esters or retinyl palmitate.

HSCs are also able to secrete cytokines, including TNFα or EGF which are essential for hepatocyte proliferation during liver regeneration. These cells can exist in two states: [1]

- Quiescent state: HSCs store vitamin A into lipid droplets;
- Activated state: HSCs act by the production of collagen I into the liver as a consequence of liver injury. Activated HSCs express αSMA, and gradually lose vitamin A [10]

1.1.4 Immune cells

The liver is also an immunological organ with a predominance of innate immunity. The liver microenvironment typically contains various cell subsets of the innate immune system, like macrophages, neutrophils, and natural killer cells, but also T and B lymphocytes that correspond to the central components of adaptive immunity. [11]

These cells have a critical role in host defense against pathogens, liver injury and repair, and tumor development. Some cells are not resident in the liver but are recruited from the bloodstream following liver injury, like neutrophils and monocytes. [12]

Lymphocytes are one of the body's main types of immune cells. They are white blood cells that are present in the bloodstream. They produce immune surveillance roles by patrolling blood, lymph nodes, and other lymphoid organs. Once Naïve T cells go in contact with APC, they are activated and migrate to the site of infections. T cells go to clonal expansion and differentiation into effector cells that can migrate to the site of inflammation. Normally, they express CCR7 and CD62L molecules on the surface. These cells are divided into memory CD8+ T, unconventional T cells as NK T cells, and lymphoid cells. [13]

Natural Killer Cells (or NK cells) are large granular lymphocytes. These cells comprise about one-half of all lymphocytes within the liver. They are phenotypically defined as CD3- CD56+. They contain granules with cytotoxic molecules like perforin or granzymes. The main function is to screen the self-molecules by the interaction of the inhibitory receptor with Major Histocompatibility Complex class I (MHC I). If it lacks there is an activation of natural killer acting as killing cells inducing apoptosis i.e. activated HSC in fibrosis regression. [14]

Neutrophils are the most abundant white blood cells in mammals. They correspond to about the 60-70% of leucocytes in peripheral blood. They are the first line of innate defense against pathogens or other danger signals. Since they have short life there is a continuous replenishment by the bone marrow. [15] In circulation mature neutrophils have an average diameter of 7-10 μm. The nucleus is segmented and the cytoplasm is enriched by different granules. Specifically, there are three types of granules:

- Primary granules (or azurophilic), which contain myeloperoxidase (MPO);
- Secondary granules (or specific), which contain lactoferrin;
- Tertiary granules (or gelatinase), which contain matrix metalloproteinase 9 (MMP9). [16]

In presence of an injury to the liver, they infiltrate from the bloodstream, but if this migration occurs in an excessive way they can produce chronic inflammation, limiting the repair of tissues and producing a loss of organ function. On the other hand, they have also a role at the end of inflammation by the production of anti-inflammatory and pro-resolving lipid mediators. They act by the production of ROS, cytokines release, and degranulation. After their role is concluded, they undergo apoptosis and a portion return to the bloodstream. [17] [18]

Monocytes are blood cells belonging to the innate immunity. Their functions are to maintain vascular homeostasis, and respond to pathogens in infections by their phagocytic activity. They are able to differentiate into macrophages. They are morphologically and functionally subdivided based on the expression of CD14 and CD16 into: [19]

- Classical CD14++ CD16-, that corresponds to those expressing $Ly6C^{high}$ with a proinflammatory activity.
- Intermediate CD14 ++ CD16+;
- Non-classical CD14+ CD16++ that corresponds to those expressing $Ly6C^{low}$;

Normally, in case of damage, they differentiate in situ into tissue macrophages and dendritic cells migrating into tissue and increasing markedly the pool of macrophages present in the injured organ. [19]

1.2 Liver fibrosis

1.2.1 Aetiology

Chronic liver disease is one of the most widespread global health problems that causes about 2 million deaths every year. [20]

Liver fibrosis is a complex fibrogenic and inflammatory process derived from a series of chronic injuries. They produce a chronic inflammation that results in an abnormal wound healing response. This process can be reversed by the remotion of the chronic source that produces the injury. If untreated, this pathology can develop into cirrhosis, an irreversible state in which the tissue is permanently damaged. Furthermore, it can worsen leading to hepatocellular carcinoma, liver failure, and death. [21]

The fibrosis process derives from the unbalance of two processes occurring as a consequence of an inflammatory cascade activated by liver injury. Firstly, the increased extracellular matrix (ECM) deposition is due to myofibroblasts activation. Secondly, the decreased degradation of ECM is due to the blockage of metalloproteinases (MMPs), by their inhibitors, Tissue Inhibitors Metalloproteinases (TIMPs). [20]

The main causes of this pathology are chronic viral hepatitis C and B, Non-alcoholic fatty liver disease (NAFLD), alcoholic liver disease (ALD), and cholestatic and autoimmune liver disease. [22]

Chronic hepatitis C and B (HCV and HBV) are chronic viral infections that affect millions of people worldwide. In particular, HCV affects about 70 million people of which 20-30% develop liver cirrhosis. HBV affects about 260 million people worldwide by vertical transmission (mother-son), especially in Africa and Asia, which lead to a chronic outcome. The mechanism of inflammation starts by the replication of the virus in hepatocytes that induce hepatocyte cell death releasing DAMPs and proinflammatory cytokines that directly activate HSCs. [22]

Non-alcoholic fatty liver disease (NAFLD) affects about 15-30% of the global adult population. Normally, it develops to NASH and the pathogenesis is composed of steatohepatitis, ballooning degeneration. The leading role that activates HSCs is the presence of oxidative stress and inflammation, that is accelerated by insulin resistance.

Moreover, the high levels of oxidative stress hamper the physiologic regenerative proliferation of mature hepatocytes. [23]

Alcoholic liver disease (ALD) is the major cause of liver fibrosis worldwide. The cause is a chronic alcohol intake that triggers several pathways to produce proinflammatory cytokines and HSCs activation. Alchohol, in hepatocytes, is metabolized into acetaldehyde, causing ROS release, secretion of TGFbeta, phagocytosis of apoptotic Kupffer cells and hepatocyte apoptosis. Moreover, this mechanism induces also the suppression of innate immunity. [22]

1.2.2 Liver fibrosis process

The extracellular matrix (ECM) is a complex network that gives mechanical support to an organ and gives mechano-elastic properties. It has a very important role in modulating the tissue homeostasis and regeneration capacity. The components of ECM are many i.e. collagens, elastin, cell-adhesion glycoproteins, glycosaminoglycans, proteoglycans, and matricellular proteins. [24]

In healthy liver, ECM compose about 10% of the total volume and normally is restricted to portal tracts, sinusoidal walls, and the central vein. During chronic liver damage, dramatic changes in ECM occurs by the increase in its synthesis and deposition, especially of the isoform collagen type I, type III, fibronectin, and laminin that can depose in the Space of Disse. [24] This is due also to the inbalance of metalloproteinases (MMPs) and tissue metalloproteinases inhibitors (TIMPs). [10] MMPs are zinc-dependent endopeptidases that are the major enzymes responsible for the degradation of ECM components and during the fibrotic process, they are downregulated in favor to their inhibitors that induce the progression of the disease. [25] (*Figure 6*)

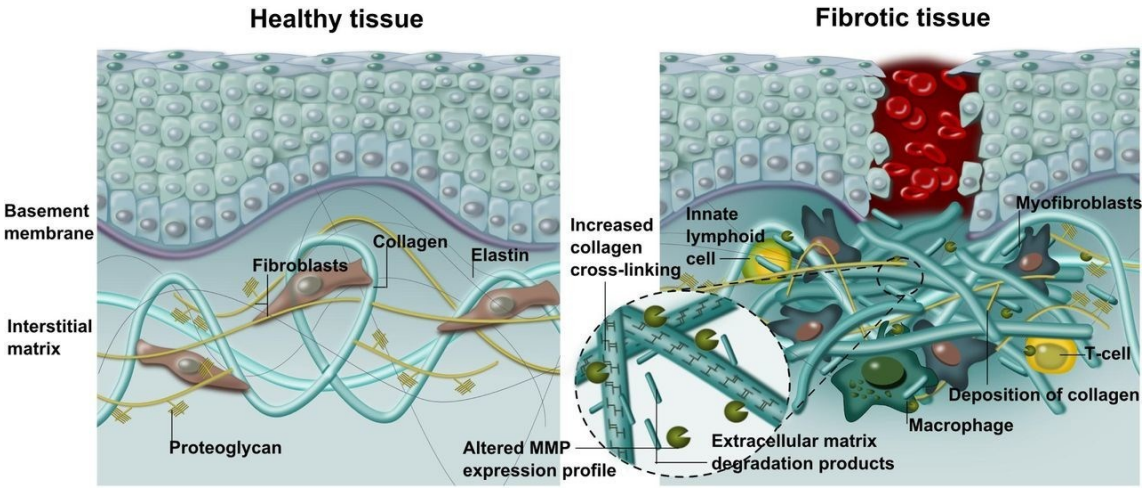

Figure 5 Difference in composition of liver parenchyma between healthy and fibrotic tissues

The key step of the fibrogenesis is the activation of HSCs that transdifferentiate into myofibroblasts. They are the main source of ECM so they have an essential role in the development and progression of fibrosis. [26] In fact, in normal healthy liver, Hepatic Stellate Cells are quiescent but in response to profibrotic stimuli become active and acquire novel features such as proliferation, contractility, enhanced ECM synthesis, chemotaxis, and generation of inflammatory signals. [10]

HSCs have also interplay with resident macrophages (Kupffer cells) and infiltrated macrophages. Macrophages secrete various proinflammatory cytokines and chemokines that trigger the activation of HSCs. The most important factors are TGFbeta, TNFalpha, IL1beta and CCL2. In particular, TNF alpha and IL1beta enhance the proliferation of myofibroblasts via the activation of the NFkB pathway. The activation of HSC produces a change in the proteins expressed with an increment of alpha-SMA protein. [10] *(Figure 7)*

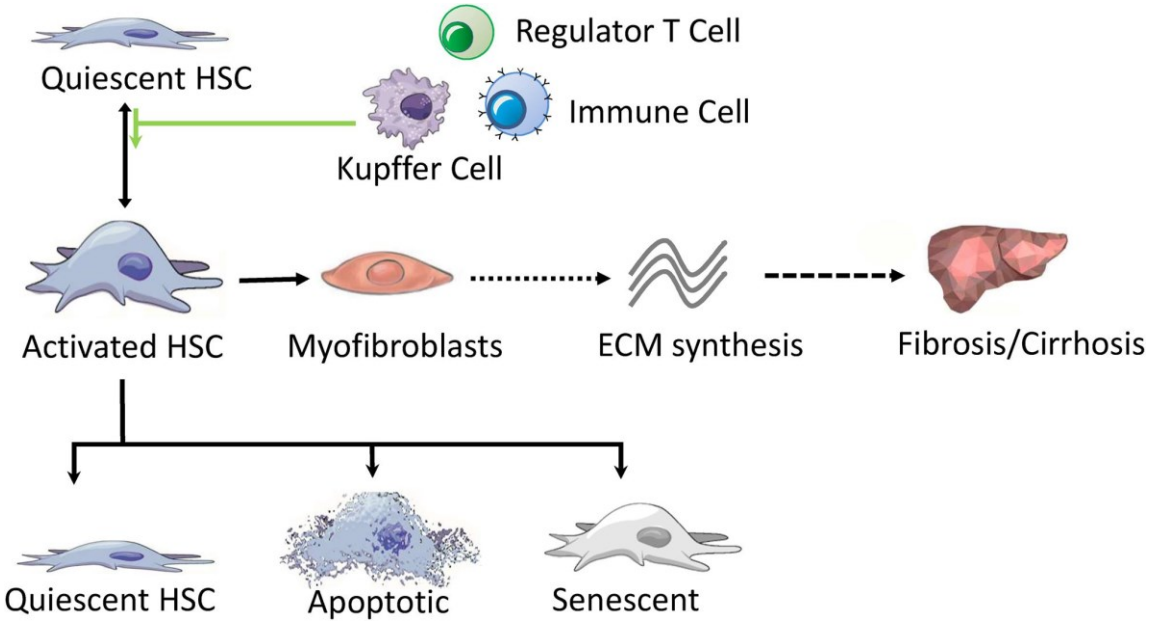

Figure 6 *Process of activation and inactivation of HSCs in fibrogenesis and regression*

The hepatic macrophages are composed of two phenotypes. The imbalance between these phenotypes mediates the progression and resolution of the inflammation. M1 phenotype, which is classically activated, has a role in the progression of fibrosis by the production of inflammatory cytokines. On the other hand, the M2 phenotype, which is alternatively activated, has a role in the resolution of fibrosis. During early damage of the liver there is an intensive recruitment of monocyte-derived macrophages mostly in the M1 isoform. The production of proinflammatory cytokines after the infiltration triggers the activation of HSCs. [10]

1.2.3 Liver regeneration process

The removal of the main inducer of chronic inflammation produce the regression of fibrosis. The regression process is formed by 3 main steps: modulation of inflammation by depletion of recruited immune cells and inflammatory cytokines i.e. IL6, IL1beta, TNF and TGFbeta, apoptosis of activated HSCs, and degradation of ECM. [27]

The main step of liver fibrosis regression is the apoptosis of activated HSC that is orchestrated by a complex interaction between pro-apoptotic and pro-survival signals. These signals produce apoptosis of about 50% of aHSC. Other HSC can return to a

quiescent-like stadium. To obtain the apoptosis several mechanisms can occur, including activation of death receptor-mediated pathways and upregulation of pro-apoptotic proteins. Hence, immune cells have a role also in the regression of liver fibrosis. Particularly, NK cells exhibit an antifibrotic activity by mediating HSCs apoptosis through the interferon gamma production, while Pro-fibrogenic Ly6C^{high} macrophages play a pivotal role in fibrosis regression by switching their phenotype to an anti-fibrogenic one. Briefly, these cells switch from a M1 polarization with pro-fibrogenic abilities to an M2 phenotype, acquiring anti-fibrogenic properties by inducing HSCs apoptosis and producing MMP9, growth factors and anti-inflammatory factors. The degradation of ECM increases due to the increasing expression of MMP9. Furthermore, the release of IL6 and TNF alpha occurs, that promote the transition of hepatocytes to mitotic cycle and their proliferation, to replace the damaged tissues and re-establish an healthy parenchyma.

1.2.4 Gender-related difference in liver diseases

The liver in mammals is a sexual dimorphic organ, by which the progression and the outcome of liver diseases is different in the two genders. [28] Moreover, it shows a gender related difference also in its composition i.e. in the number of Kupffer cells and hepatocytes. Epidemiological studies show sex-related differences in various liver diseases. Particularly, NAFLD and NASH show a higher incidence in men than in women. In particular, a Japanese study showed a 24% prevalence of NAFLD in men, 6% in a pre-menopausal woman that increased to 15% after menopause. So, women show a reduced risk of NAFLD development during their fertile age. [23] Since gender can impact the development and treatment of chronic diseases it is essential to perform additional preclinical and clinical studies to obtain a broader appreciation of fibrosis mechanisms, progression and therapy.

Nowadays, there is an incoming hypothesis of a sex-related dimorphism in innate immunity. Evidences show a disparity in the immune response between males and females. Females are more prone to produce both innate and adaptive immune responses compared to males, also females are more prone to develop autoimmune diseases. In males was observed a higher susceptibility to infections from birth to adulthood, suggesting a role of sex chromosomes in innate immunity. Also, the sex

hormones regulate differentiation and effector function of innate immunity cells, such as neutrophils, macrophages, natural killer cells, and dendritic cells. [29]

Different studies show a difference in polarization of M1 or M2 phenotype. For example, a higher polarization to the M1 proinflammatory phenotype was observed in male mice, while females showed a higher polarization to M2, a reparative phenotype. [29]

AIM

Liver fibrosis is a pathological condition that occurs as a consequence of chronic insult to the hepatic parenchyma. The resulting process consists in the formation and deposition of abnormal amounts of scar tissue replacing the healthy ones. The key step of fibrogenesis is the activation of Hepatic Stellate Cells (HSCs) that trans-differentiate into myofibroblast-like cells, inducing the production of excessive extracellular matrix (ECM).

During liver fibrosis, the balance between the two main regulators of ECM homeostasis, i.e. metalloproteinases (MMPs) and tissue inhibitors of metalloproteinases (TIMPs), is altered. Moreover, overexpression of TIMPs by hepatic stellate cells contributes to the pathogenesis of liver fibrosis.

The injury that hit the hepatocytes in the liver activates Kupffer cells (KCs). They activate a pro-inflammatory cascade that recruits Ly6Chigh monocyte-derived macrophages (MoMFs) from the bloodstream. This subset of immune cells exert a pro-fibrotic role by inducing higher matrix secretion and deposition resulting in fibrosis progression.

Since the liver can self-regenerate, liver fibrosis could be resolute by removing the causative agent. The regenerative process mainly consists of apoptosis of HSCs, ECM degradation, and hepatocyte proliferation.

Since liver is an organ that has dimorphism, epidemiological studies show an underlined gender-related difference in the immune response against insults and regeneration mechanism. In fact, an increased immune response in females was observed, that cause a reduced susceptibility to infections. Moreover, there is an increased incidence of liver pathologies in men compared to women.

Based on these considerations this work aimed to study the mechanisms involved in fibrogenesis and regeneration in mice of both genders, especially evaluating the role of the immune cells in these processes.

In order to achieve our aim, we developed a model of progressive liver fibrosis by intraperitoneally injecting the toxic agent CCl_4 for 12 weeks to both female and male Balb/CJ mice. After that, a washout period of 8 weeks was performed to allow liver regeneration. Mice were sacrificed after 6, 12, and 20 weeks to collect their livers and perform histological, flow cytometry, and quantitative real-time PCR analysis.

MATERIALS AND METHODS

2.1 Treatment of mice with CCl_4

All the experiments were performed in agreement with the internationally accepted principle of care and use of laboratory animals (Legislative Decree No. 26/2014, which accepted and applied the European Union Directive 2010/63/EU on the protection of animals used for scientific purposes). The animals were housed in the animal facility in the Department of Pharmaceutical and Pharmacological Sciences, Pharmacology Building, University of Padua.

Female and male BALB/CJ mice weighing between 16 and 30 grams (approximately 8 weeks of age) were randomly divided into two groups. Group I (healthy control group) was treated with an intraperitoneal injection of corn oil, while Group II (fibrotic group) was treated with carbon tetrachloride (CCl_4) in corn oil.

Increasing doses of CCl_4 were administered twice a week for 12 weeks to lead to progressive liver damage without adaptive responses of the liver to the injury. Afterward, a washout period with no administration of CCl_4 was performed for 8 weeks. The CCl_4 treatment protocol started at week 1 with a dose of 0,17 µL/g (Figure 8) that was increased by 0,1 µL/g each week, until week 5. Then, from week 6 to week 9 the dose has been augmented by 0,05 µL/g per week. During weeks 10, 11, and 12 we administered the maximum dose of 0,72 µL/g to mice. A washout period, without CCl_4 treatment, was performed from the end of week 12 until week 20 to allow liver regeneration.

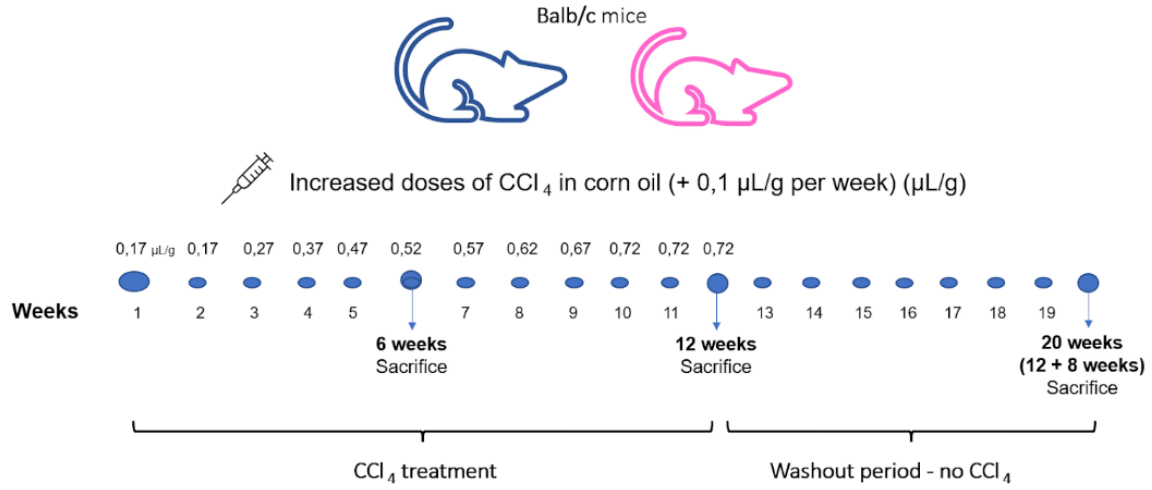

Figure 7 Treatment and washout period schedule.

Five CCl_4-treated mice and five control mice of both genders were sacrificed after 6, 12, and 20 weeks. For sacrifice, mice were anesthetized with isofluorane and the liver was perfused with saline. For liver perfusion, a butterfly catheter connected to a perfusion pump was placed in the left ventricle, while the right atrium was cut to allow blood cell elimination. After, the liver was excised and cut into three parts. The first liver portion was placed in liquid nitrogen and stored at -80°C for the RNA extraction, the second was placed in formalin (4%) for histological analysis, and the last one was posed in phosphate buffered-saline and ethylenediaminetetracetic acid mixture (5 mL of PBS, 0,1% EDTA) for flow cytometry experiments.

2.2 Ex vivo analysis

Flow cytometry analysis was performed to evaluate the relative abundance of Kupffer Cells, Neutrophils, and Ly6C^{high} Monocyte-derived Macrophages (MoMFs). Masson's Trichrome Stain was performed to assess the collagen content in livers. Immunohistochemistry was conducted for the identification of activated Hepatic Stellate Cells (HSCs) and the presence of Metalloproteinases (MMP-9) and Inhibitor of Metalloproteinases (TIMP-1). Finally, Quantitative Real-Time PCR (qPCR) was

performed to evaluate the RNA of major cytokines involved in the inflammatory and fibrogenic process.

2.2.1 Flow cytometry analysis

Immediately after sacrifice, a liver portion was placed in PBS/EDTA and processed to obtain a single-cell suspension. The protocol started by incubating the liver portion with a digestion mixture of collagenase IV 2mg/ml and DNAse I 0,005 µg/mL at 37°C for 40 minutes, allowing enzymatic digestion. Afterward, the tissue was minced into small pieces by using forceps in order to obtain a cell suspension. The obtained cell suspension was filtered with a 70µm cell strainer, washed with RPMI 10% FBS, and then centrifuged twice at 300 RCF for 5 minutes. A quantity of $1x10^6$ cells/mL was collected and incubated with Mouse Fc block for 15 minutes at room temperature to prevent unspecific binding of the antibodies. Moreover, the staining protocol was performed by using calculated dilutions of the primary antibodies in PBE (composed of 0,5% BSA, 2nM EDTA in PBS), followed by a 15-minute-incubation period at room temperature.

To stain liver cells, these antibodies were used:

1. APC-conjugated anti-mouse F4/80;
2. APC-Cy7-conjugated anti-mouse Ly6G;
3. BV711-conjugated anti-mouse CD11b;
4. SB436-conjugated anti-mouse Ly6C;
5. PE-conjugated anti-mouse CD45;
6. PE-Cy7-conjugated anti-mouse B220, NK 1.1, and CD3.

At the end of the incubation period, a final centrifuge was performed at 1200 rpm for 5 minutes. Finally, cells were diluted in formalin 4% to fix them.
A gating strategy was set to identify the populations of our interest, including Neutrophils, Kupffer Cells, and $Ly6C^{high}$ Macrophages. The cell count is expressed as the frequency of parent, meaning they are identified as percentages out of the parent population.
The flow cytometry experiment was performed with an LSRII instrument at IOV (Veneto Institute of Oncology), Padua, under the supervision of Prof. Giulia Pasqual.

2.2.2 Paraffin-embedded liver protocol

After mice sacrifice, a portion of the liver was preserved in formalin 4% for histological analysis. The liver portion was then embedded into paraffin blocks by following a protocol for the dehydration of the tissue. Each of the following dehydration steps lasted 1 hour:

- 70% Ethanol 30% Methanol solution
- 80% Ethanol 20% Methanol solution
- 95% Ethanol 5 % Methanol solution
- 100% Ethanol (repeated two times)
- Xylene (repeated two times)

In the end, the tissue was included using liquid paraffin which has been previously warmed.

2.2.3 Masson's Trichrome Stain

Masson's Trichrome Stain was performed to assess the phenotype of the liver and highlight fibrotic scars. Collagen fibers were stained in green, cell cytoplasm was stained in red, and the nuclei were counterstained in violet with hematoxylin. Five µm-thick slices were cut from the paraffin blocks by using a microtome. The staining was conducted by using the "Masson-Goldner staining kit" (Sigma-Aldrich).

The sections were firstly deparaffinized following this protocol: incubation in xylene with 3 changes (5 minutes each), 95% ethanol with 3 changes (5 minutes each), and dips in distilled water.

The slices were then incubated in Bouin's solution for 30 minutes at 37°C and rinsed in stained with Harry's Hematoxylin for the identification of cell nuclei. Afterward, the slices were dipped in acid ethanol and ammonia solution to fix the staining of hematoxylin. In the end, slices were stained with azophloxine solution for cytoplasm staining, tungstophosphoric acid Orange G solution for erythrocytes, and light green SF solution for connective tissue. Each staining step was followed by washes in 1% acetic acid solution.

Sections were dehydrated in acid ethanol (1 minute), in alcohol for two times (respectively for 30 seconds and 1 minute) and in xylene for two times (5 minutes each one). In the end, slices were covered with a coverslip using a drop of Eukitt mounting medium and examined with an Optika Microscope (Italy).

2.2.4 Immunohistological localization of α-SMA, MMP-9, TIMP1

Five μm-thick slices from paraffine blocks were cut by a microtome. Then, the slices were deparaffinized as described above *(par. Masson's Trichrome Stain)* and incubated with antigen retrieval solution (*see Table 1)* for 25 minutes at 95°C.

Since αSMA is an intracellular protein, (MMP9 and TIMP1 are extracellular agents and they do not require the permeabilization step) slices were permeabilized with Tryton x 100 0,2% for 10 minutes at room temperature. Afterward, slices were washed and incubated for 30 minutes with 5% fetal bovine serum (FBS) to block unspecific binding.

Sections were incubated overnight at 4°C with the primary antibody directed against the different targets of our interest *(see Table 1).* The day after, slices were washed three times in PBS and incubated at room temperature with 0,3% H_2O_2 for 15 minutes to inhibit endogenous peroxidases. Moreover, slices were incubated with an HRP-conjugated secondary antibody for 1 hour at 37°C in a dark environment (*see Table1*). Finally, slices were stained with a solution of DAB and tris-HCl (H 7,6) (3,3'-diaminobenzidine) for 10 minutes, followed by a counterstaining with Harris Hematoxylin.

Sections were dehydrated in 95% ethanol three times and then in xylene for three times. The slides were covered by coverslips with Eukitt mounting medium and analyzed by using an Optika Microscope (Italy).

Protein	**Antigen retrieval**	**Primary ab**	**Secondary ab**
α-sma	Tris-EDTA	Rabbit α-sma	Anti-rabbit
Mmp9	Citrate	Mouse Mmp9	Anti-mouse
Timp1	Citrate	Rat Timp1	Anti-rat

Table 1 Types of antibodies used for α-SMA, MMP9, and TIMP1 protein with IHC analysis

2.2.5 RNA extraction

Liver RNA was extracted from frozen tissue using the Animal Tissue RNA Purification Kit (Norgen), following the manufacturer's instructions. Briefly, 15 mg of frozen liver tissue were homogenized in a 1,5 mL Eppendorf with Buffer RL and β-mercaptoethanol. Then, 600 µL of RNAse-free water and 20 µL of Proteinase K were added to the lysate and incubated at 55°C for 15 minutes to disrupt the tissue proteins, including collagen and contractile proteins.

The obtained suspension was centrifuged and 450 µL of 96-100% ethanol was added to the supernatant. After centrifugation, the supernatant was loaded on a column assembled with a specific collection tube. Wash Solution A, Enzyme Incubation Buffer A, and 15 µL of DNase I were separately applied to the column, and each step was followed by centrifugation. Finally, 50 µL of Elution Solution A was applied to the column, followed by two consecutive centrifugations. The resulting elution product was the purified RNA sample that was immediately stored at -80 °C. RNA concentration and purity were measured by a Nanodrop spectrophotometer.

2.2.6 Real-time time PCR

The RNA extracted was used to measure the expression of the following genes: COL1A1, TGFβ, TNFα, PDGF, CCL2, VEGFA by using a qRT-PCR technique with "QuantiNova ® SYBR ® Green RT-PCR Kit (Qiagen).

The primer sequences of each gene that were used for the amplification of the cDNA were reported in *Table 2*. Samples were loaded in triplicate in a 96-well plate with 3.9 µL of RNA and 6.1 µL of Mastermix for each well. The composition of each well is exemplified in *Table 3.* In the end, the plate was fulfilled, sealed, and centrifugated for 1 minute at 1000 RPM. The qRT-PCR was conducted by using a 7500 fast real-time PCR system (Bio-rad).

Gene	**Forward primer (5'-3')**	**Reverse primer (3'-5')**
Col1a1	AGC ACG TCT GGT TTG GAG AG	GAC ATT AGG TGC AGG AAG GT
VEGF	ACT GGA CCC TGG CTT TAC TG	CTC TCC TTC TGT CGT GGG TG
Tgfβ	GTG GAA ATC AAC GGG ATC AGC	GTT GGT ATC CAG GGC TCT CC
Tnfα	CCC ACG TCG TAG CAA ACC A	TGT CTT TGA GAT CCA TGC CGT
Pdgfa	CTG TGT TCC TCT GCC CCT TT	TGT CAT GTC TCC ATG CTG C
Ccl2	CCA CAA CCA CCT CAA GCA CT	AGG CAT CAC AGT CCG AGT CA
βactin	AGC AAG CAG GAG GAT GAG	AAA ACG CAG CTC AGT AAC AGT

Table 2 Primer sequences that were used to perform qRT-PCR

Reagents	**Volume in µL per well**
2x quantinova sybr green	5
Quantinova sybr green reverse transcriptase	0.1
Primer for+rev (both 10µM)	1
RNA diluted with RNAse-free water	3,9

Table 3 Quantification of master mix and RNA per well.

2.2.7 Data analysis and statistics

The statistical analysis was performed by using the GraphPad Prism software, ver. 6.0. The statistical difference among the experimental groups was calculated using Student's t-test or one-way ANOVA, when appropriate. Unless otherwise stated, data are expressed as mean ± standard error of the mean (SEM). A P value < 0.05 was considered statistically significant.

RESULTS

3.1 Masson's Trichrome Stain

The Masson's Trichrome stain was used to assess the severity of liver fibrosis by staining collagen fibers in green, while erythrocytes and cell cytoplasm were stained in orange and red, respectively. Control mice (treated with oil) showed normal architecture of the liver and the absence of fibrotic septa. After 6 weeks of treatment with CCl_4 mice of both genders showed an initial development of fibrotic septa, while after 12 weeks hepatic fibrosis became more evident, showing a worsening of the condition. In the end, after the recovery period, a decrease in collagen content on fibrotic septa was observed, even if fibrotic scars were still present. (*Figure 9*)

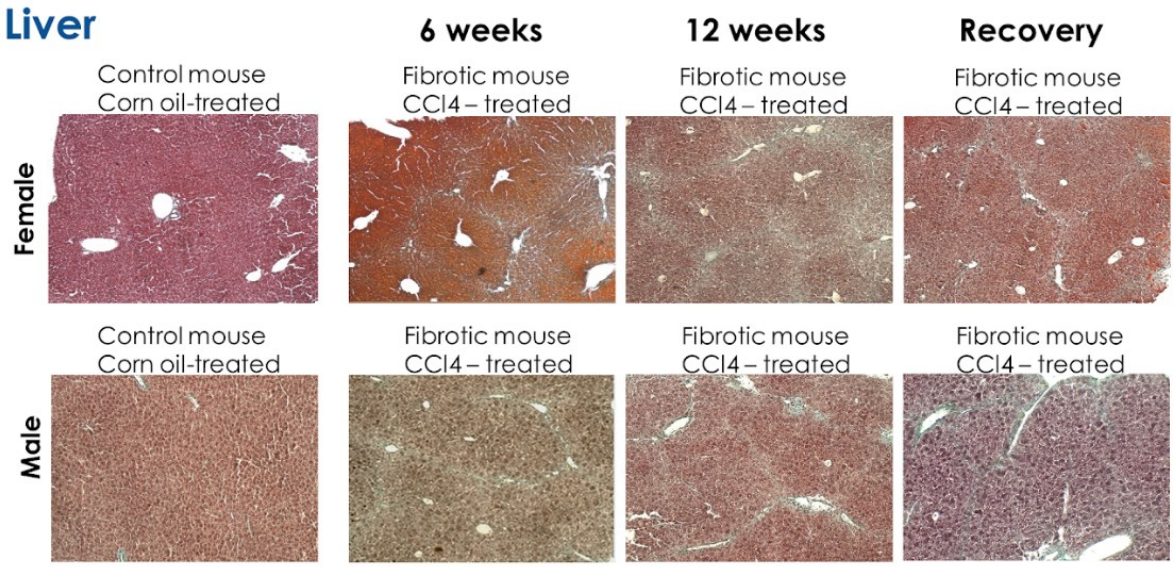

Figure 8 ***Masson's trichrome stain****. Representative images of Masson's trichrome stain of livers at weeks 6, 12, and after the recovery period for both male and female mice (magnification 10x).*

The collagen evidenced by Masson's Trichrome Stain was quantified by ImageJ software and the obtained values were expressed as percentages of collagen fibers out of the total image that was acquired. (*Figure 10*)

The collagen areas were higher in CCl_4-treated mice compared to controls for both genders, at each time point (6 weeks, 12 weeks, and Recovery).

After 6 weeks of treatment, the collagen area was higher in males compared to females. On the other hand, after 12 weeks of CCl_4 treatment, no differences between genders were observed, and after the recovery period collagen areas massively decreased in fibrotic female mice.

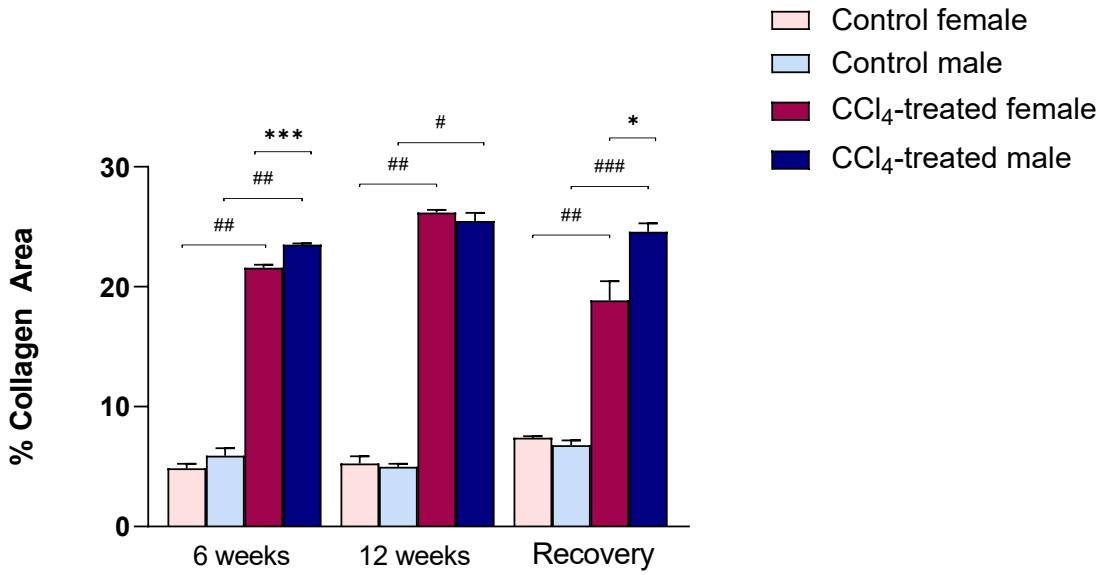

Figure 9 ***Quantification of collagen area.*** *The histogram represents the percentage of collagen area after 6 and 12 weeks of treatment and recovery. Data are presented as mean ± SEM of 5 images for each mouse (n=5 per group); #p<0,05, ##p<0,01, ###p<0,001 vs. control*

3.2 Immunohistochemical localization of α-SMA, MMP9, TIMP1

3.2.1 α-SMA

The key step of the fibrogenic process is mediated by the activation of Hepatic Stellate Cells (HSCs), which induces the abnormal deposition of extracellular matrix (ECM) that replaces the normal tissue. The α-smooth muscle actin (α-SMA) marker is peculiar to HSC activation. [21]

α-SMA+ areas were analyzed by using ImageJ software and values were expressed as percentages of α SMA+ areas out of the total image that was acquired.

α-SMA was evident only around the blood vessels of livers from control groups. However, after 6 and 12 weeks of CCl_4-treatment, there was a significant presence of αSMA in fibrotic mice of both genders. (*Figure 11)*

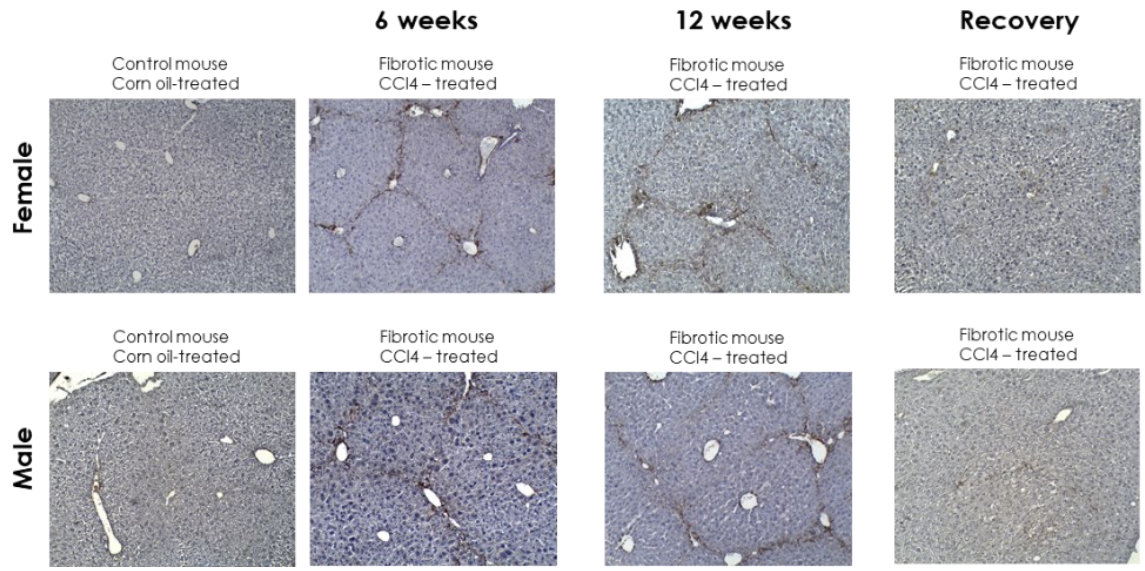

Figure 10. ***Immunohistochemical localization of αSMA****. Representative images (magnification 10x) of αSMA expressed in liver tissue after 6 and 12 weeks of treatment and recovery period in both male and female mice.*

After 6 and 12 weeks α-sma positive areas were significantly higher compared to control groups, while returned to physiological levels in the recovery period.

In particular, females treated with CCl_4 showed a gradual increase between the 6 and 12 weeks and returned equally to controls during recovery, while males showed a huge increase after 6 weeks, but after 12 weeks there was no difference between genders. After the recovery period and despite the damage being dismissed, fibrotic male mice showed a small amount of αSMA positive areas, while in fibrotic female mice the levels of activated HSCs were comparable to control groups. (*Figure 12)*

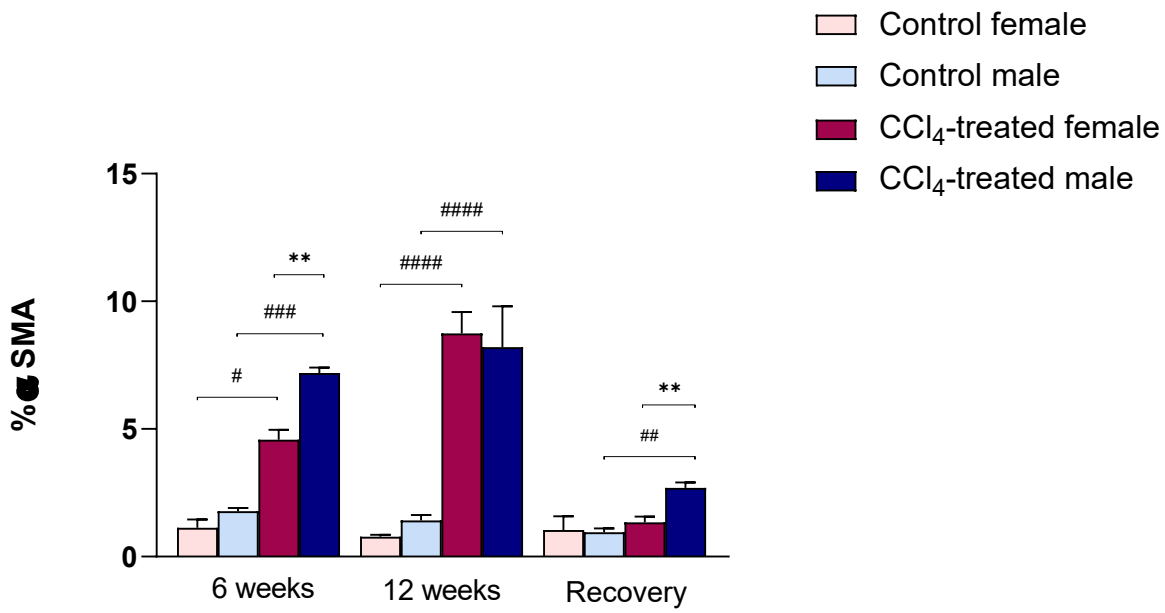

Figure 11 ***Quantification of αSMA of female mice (A) and male mice (B).*** *The histogram represents the percentage of αSMA of weeks 6, 12, and recovery. Data are presented as mean ± SEM of 5 images for each mouse (n=5 per group); #p<0,05, ##p<0,01, ###p<0,001, ####p<0,0001 vs. control*

3.2.2 MMP9

MMP9 is the most present metalloproteinase (MMP) during the regression of liver fibrosis, and it is mainly produced by KCs and Ly6Chigh macrophages. During liver fibrosis MMPs are still present but their expression is reduced, resulting in reduced degradation of ECM, while during the regression of liver fibrosis increase its expression, obtaining a reactivation of its activity. [25]

MMP9+ areas were analyzed by using ImageJ software and values were expressed as percentages of MMP9+ areas out of the total image that was acquired.

Immunohistochemistry on liver tissues revealed that the presence of MMP9 in both genders from control and CCl_4-treated mice was mostly around the vessels. *(Arrow in Figure 13).*

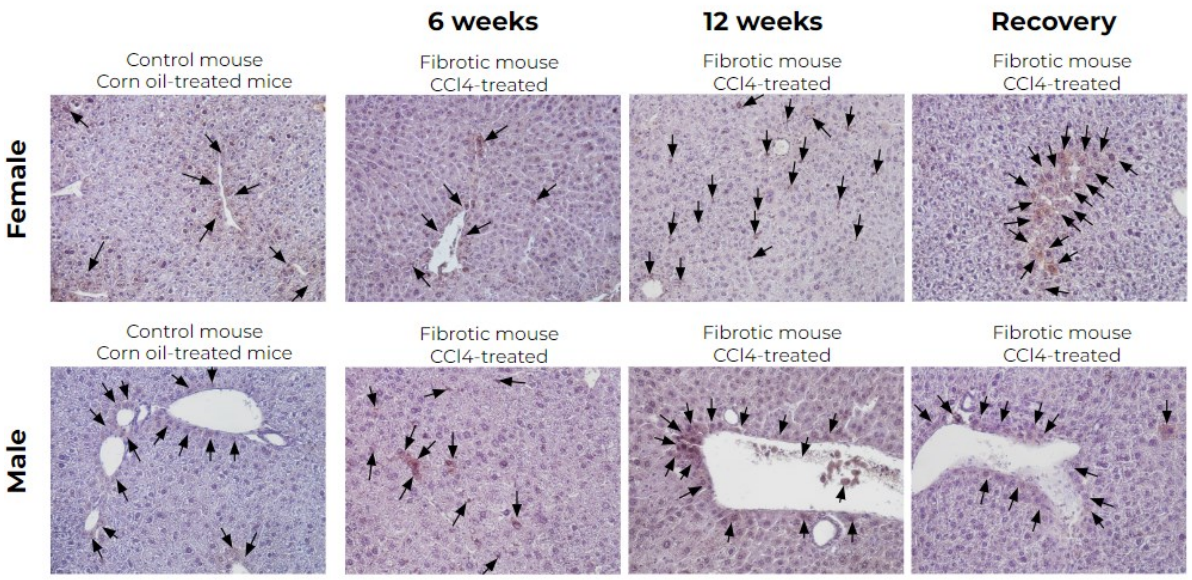

Figure 12. ***Immunohistochemical localization of MMP9****. Representative images (magnification 10x) of MMP9 expressed in liver tissue after 6 and 12 weeks of treatment and after the recovery period in both male and female mice.*

Our analysis of MMP9 revealed that after 6 weeks of CCl_4 treatment MMP9 levels in fibrotic mice from both genders were lower than in control mice, while no differences were observed after 12 weeks. After the recovery period, a huge increase in MMP9 levels was observed in fibrotic mice of both genders, especially in fibrotic female mice, with respect to control mice. *(Figure 14)*

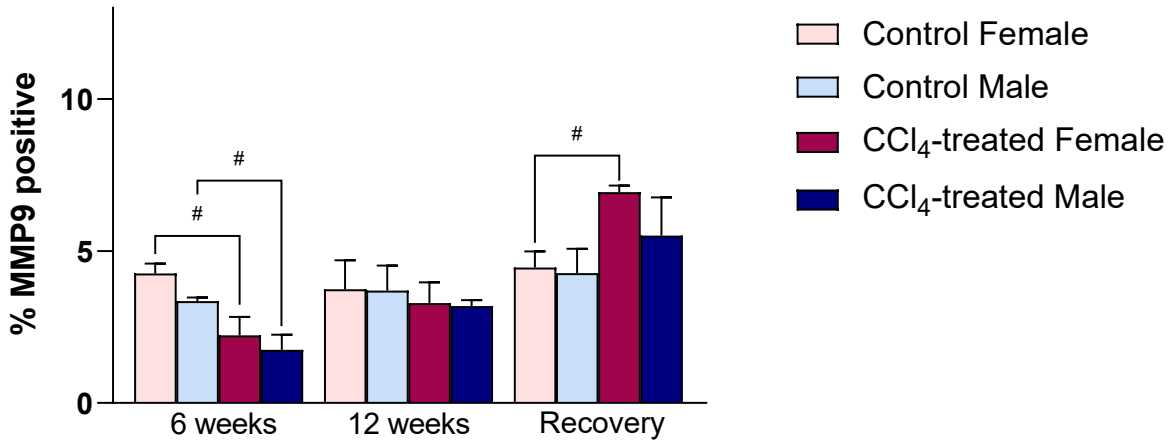

Figure 13 ***Quantification of MMP9 of female mice (A) and male mice (B).*** *The histogram represents the percentage of MMP9-positive mice for weeks 6, 12, and*

recovery. Data are presented as mean ± SEM of 5 images for each mouse (n=5 per group); #p<0,05 vs CCl4-treated mice of the same gender..

3.2.3 TIMP1

TIMP1 (Tissue Inhibitor of Metallo Proteinases 1) is a specific endogenous inhibitory protein belonging to the TIMP family. The functions are accounted for inhibiting the matrix metalloproteases (MMPs). Their action is to promote liver fibrosis by regulating the activity of MMPs. [9]

Immunohistochemistry on liver tissues revealed that the presence of TIMP1 in both genders from control and CCl_4-treated mice was mostly around the vessels. *(Figure 15)*

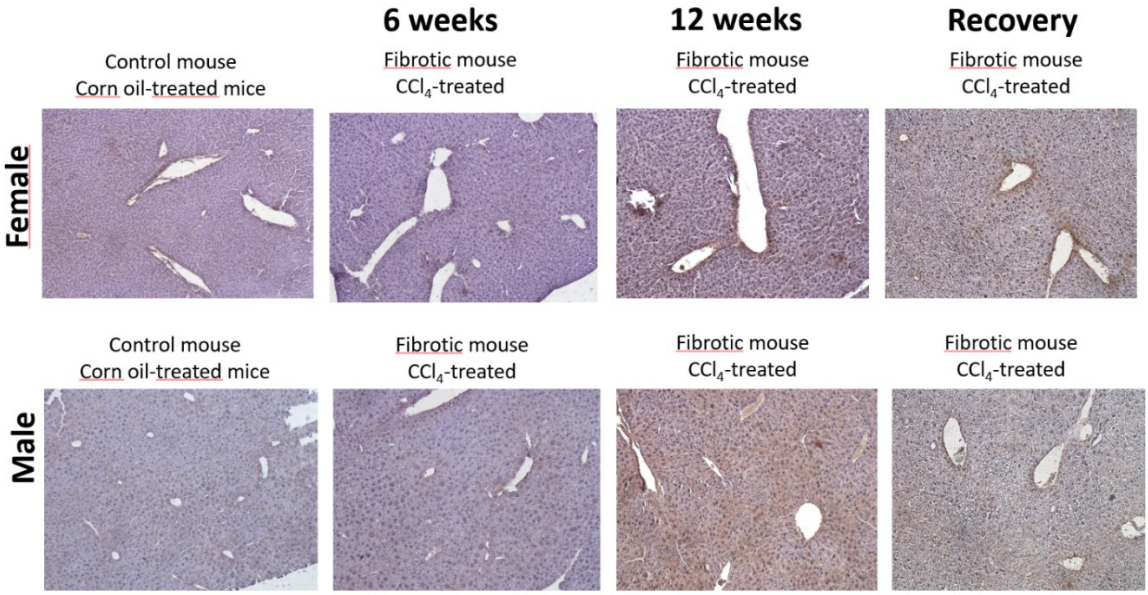

Figure 14 ***Immunohistochemical localization of TIMP1****. Representative images (magnification 10x) of TIMP1 expressed in liver tissue after 6 and 12 weeks of treatment and recovery period in both male and female mice.*

TIMP1+ areas were analyzed by using ImageJ software and values were expressed as percentages of TIMP1+ areas out of the total image that was acquired.

After 6 weeks we noticed a big increase in TIMP1 levels in CCl_4-treated mice of both genders, with respect to control mice. TIMP1+ areas were higher in males than females, showing sex-related differences in the onset of the disease. After 12 weeks there was a further increase of TIMP1+ areas in fibrotic females, while TIMP1 levels remained stable

in fibrotic male mice. After the recovery period, TIMP1 levels decreased in CCl_4-treated mice of both genders, showing sex dimorphism in the levels of this enzyme. In particular, during liver regeneration, the levels of TIMP1 in fibrotic males were still high, and higher than in fibrotic females (*Figure 16*).

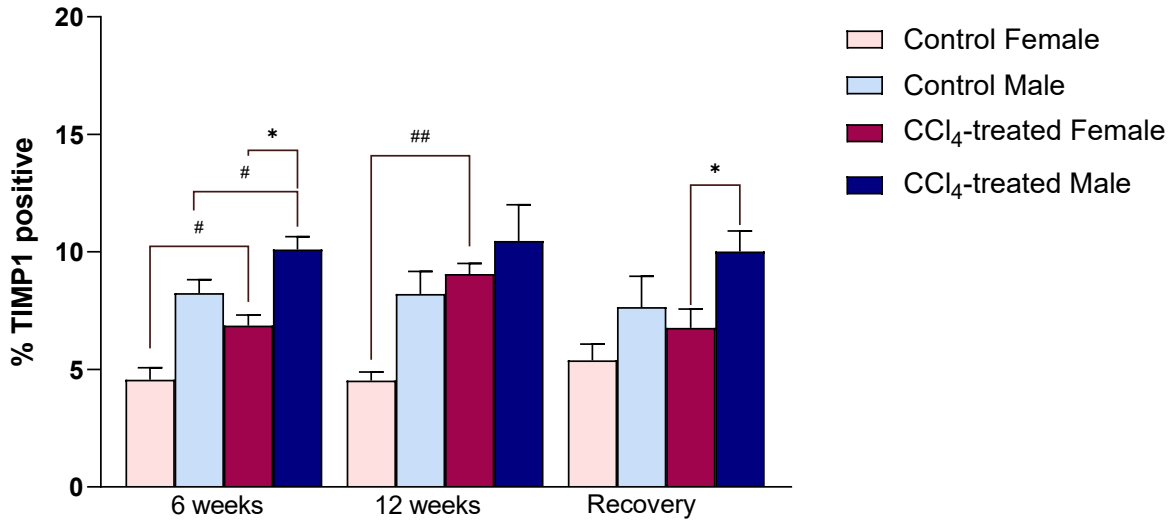

Figure 15 ***Quantification of TIMP1 of female mice (A) and male mice (B).*** *The histogram represents the percentage of TIMP1-positive cells in mice for weeks 6, 12, and recovery. Data are presented as mean ± SEM of 3 images for each mouse (n=3 per group); #p<0,05, ##p<0,01.*

3.3 FLOW CYTOMETRY

3.3.1 NEUTROPHILS

Neutrophils were analyzed by flow cytometry as CD11b+ Ly6G+ cells.

Gating strategy: First, CD45+ cells were selected (A), then the CD11b positive and Ly6G positive were gated and quantified (B). (*Figure 17*)

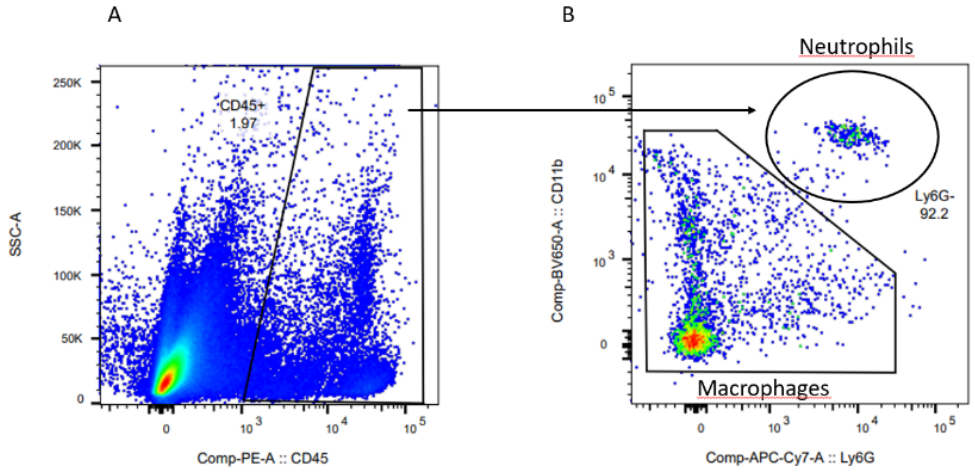

Figure 16 Gating strategy for the identification of neutrophils

The analysis revealed that after 6 weeks there was a huge increment in fibrotic mice of both genders, with more recruited neutrophils in fibrotic females than males. After both 12 weeks and the recovery period, the quantity of Ly6G+ cells returned almost to basal levels. *(Figure 18)*

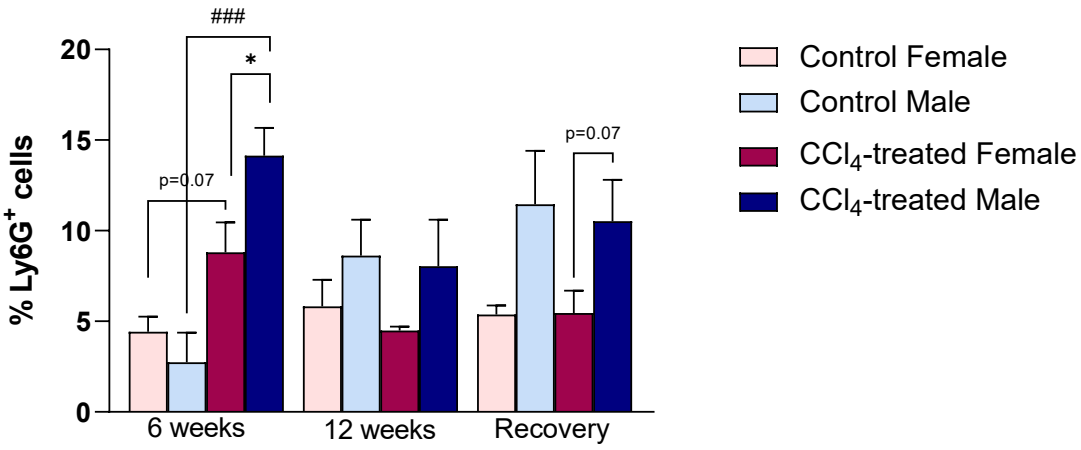

Figure 17 ***Quantification of neutrophils of female mice (A) and male mice (B).*** *The histogram represents the percentage of Ly6G$^+$ cells in mice at weeks 6, 12, and recovery. #p<0,05, ##p<0,01, ###p<0,001 vs. control mice of the same gender.*

3.3.2 LYMPHOCYTES AND NK

Lymphocytes and natural killer cells were selected by the identification of $CD3^+$ $B220^+$ and $NK1.1^+$ cells.

Gating strategy: First, we select CD45+ cells (A), Neutrophils were identified and excluded (CD45+ CD11b+ Ly6G+ cells), while CD45+ CD11+ Ly6G- cells were gated (B). From this gate, we selected double positive cells for both CD11b and CD3, B220, and NK 1.1 (C). (*Figure 19)*

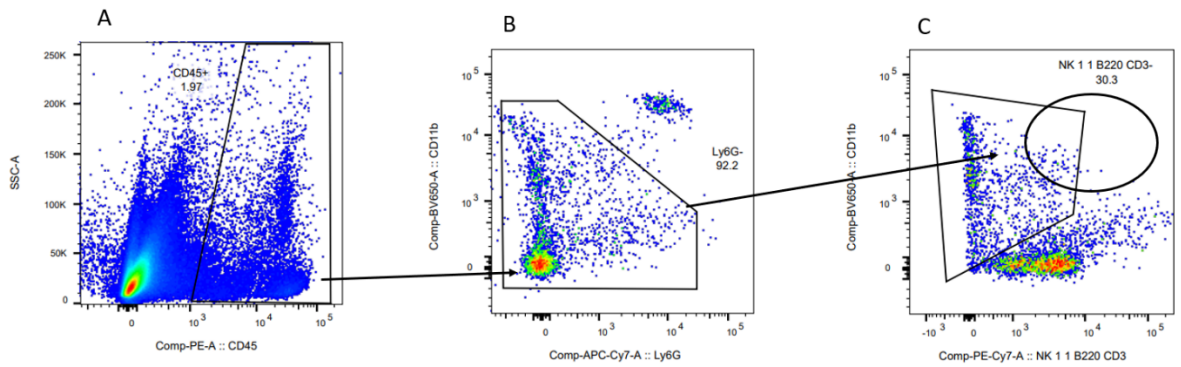

Figure 18 Gating strategy for the identification of lymphocytes and NK cells

In fibrotic males, the levels of lymphocytes and NKs were constant among the different time points, with no significant differences with respect to control male mice. On the other hand, although fibrotic females had similar levels of $CD3^+$, $B220^+$, and $NK1.1^+$ cells as well as their healthy counterparts, during liver regeneration the levels of these cells were

massively increased. However, we were not able to distinguish lymphocytes from NKs because we did not selectively stain lymphocytes and NKs. *(Figure 20)*

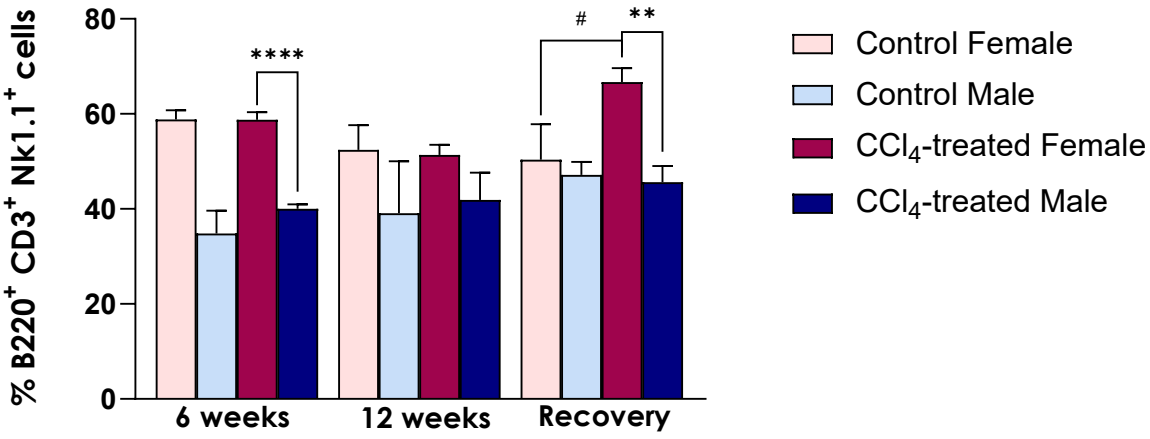

Figure 19 ***Quantification of lymphocytes and NK cells of female mice (A) and male mice (B).*** *The histogram represents the percentage of B220+, CD3+, and Nk1.1+ cells in mice at weeks 6, and 12 and recovery. Data are presented as mean ± SEM #p<0,05, ##p<0,01, ###p<0,001, ####p<01 vs. control mice of the same gender.*

3.3.3 KUPFFER CELLS

To identify the resident macrophages (Kupffer Cells) was developed a gating strategy that identifies the population CD11b^{int} F4/80 ^{high}.

Gating strategy: First, CD45-positive cells were gated (A). As in the previous gating strategy, neutrophils were identified (CD45+ CD11b+ Ly6G+ cells) and excluded. Consequentially, the gating strategy proceeds by selecting CD45+ CD11b+ Ly6G- cells (B). Lymphocytes and NKs (CD11b+ CD3+ B220+ NK1.1+) were identified and excluded, and a gate on CD11b+ CD3- B220- NK1.1- were created (C). Double positive cells for CD11b and F4/80 were included, but specifically, Kupffer cells were selected by choosing the CD11b^{int} and F4/80 ^{high} cells (D). *(Figure 21)*

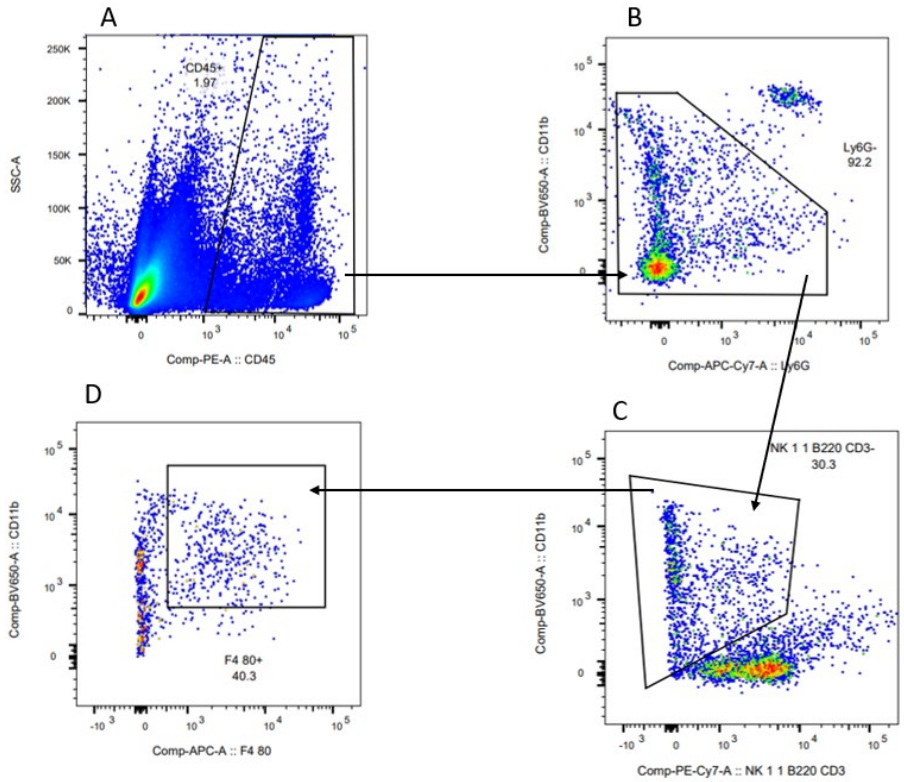

Figure 20 Gating strategy for the selection of Kupffer cells

At every timepoint, fibrotic mice of both genders had lower levels of KCs than control mice. After 6 weeks of treatment, the levels of KCs in female fibrotic mice were comparable to fibrotic male mice. After 12 weeks, the quantity of KCs massively decreased in fibrotic mice from both genders, with no significant sex-related differences. After the recovery period, the levels of KCs increased in fibrotic mice of both genders, with higher levels in fibrotic males than in fibrotic females. (*Figure 22)*

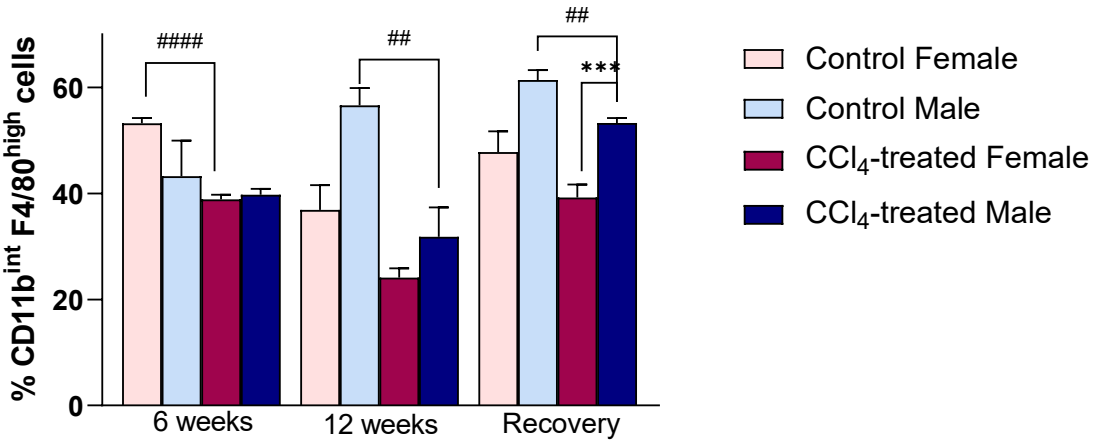

Figure 21 ***Quantification of Kupffer cells of female mice (A) and male mice (B).*** *The histogram represents the percentage of CD11b^{int} F4/80^{high} cells on mice at weeks 6, 12, and recovery. #p<0,05, ##p<0,01, ###p<0,001, ####p<0 vs vs. control mice of the same gender.*

3.3.4 Ly6C MACROPHAGES

Gating strategy for the identification of Ly6C^{high} F4/80$^{med\ to\ high}$ CD11b^{high} population that corresponds to infiltrating macrophages.

CD45 positive cells were gated (A). Neutrophils were identified as viable CD45+, CD11b+, and Ly6G+ cells and they were excluded from the subsequent macrophage gating, whereas cells positive for CD11b were gated (B). Cells positive for CD3, B220, and NK 1.1 (lymphocytes) were excluded. Cells positive for CD11bhigh were selected (C). Cells positive for F4/80 med to high and CD11high were gated (D). Cells positive for Ly6Chigh F4/80med to high were gated (E). *(Figure 23)*

Ly6Chigh F4/80med to high CD11bhigh identified the target population of infiltrated macrophages.

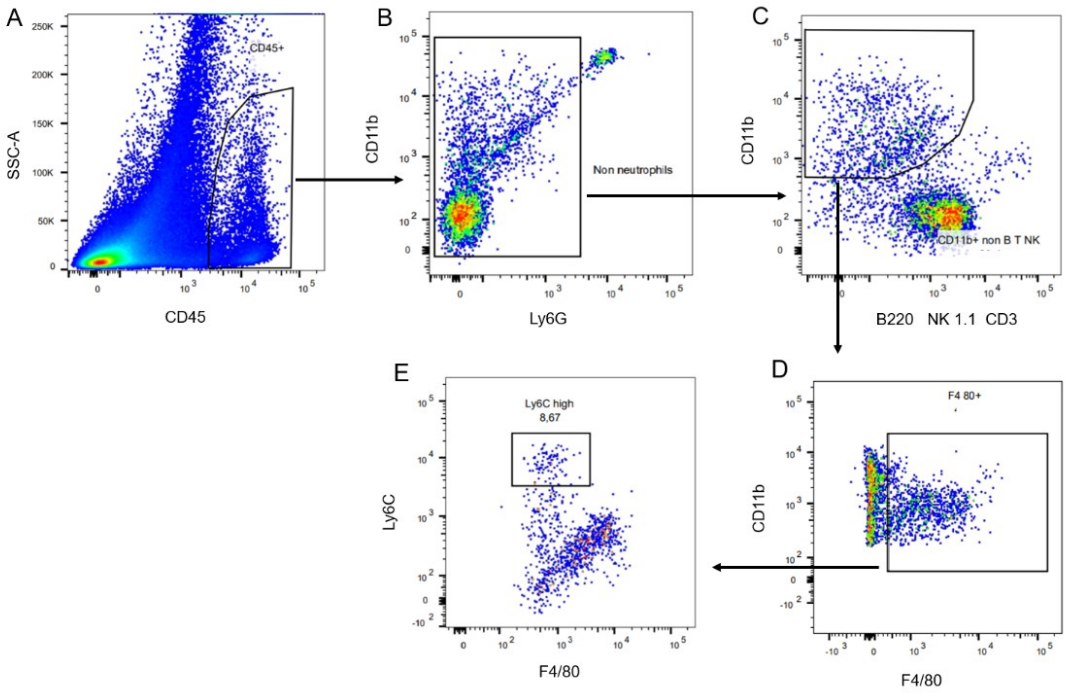

Figure 22 Gating strategy for the identification of Ly6C^{high} infiltrating macrophages

Profibrotic Ly6C macrophages are analyzed as a percentage of Ly6C ^{high} F4/80 ^{int} CD11b ^{high}.

In males, the value is higher than the control during the CCl_4 treatment. The highest pick occurs after 12 weeks of treatment and decreases gradually during the recovery of treatment, reaching the amount comparable to control in the recovery period.

In females, the value is always higher than the control during the treatment, reaching the peak at 12 weeks of treatment and decreasing to basal levels at recovery.

The difference between genders is evident at 6 weeks, with a higher quantity in males while the opposite effect could be observed at 12 weeks. This difference is maintained after recovery. *(Figure 24)*

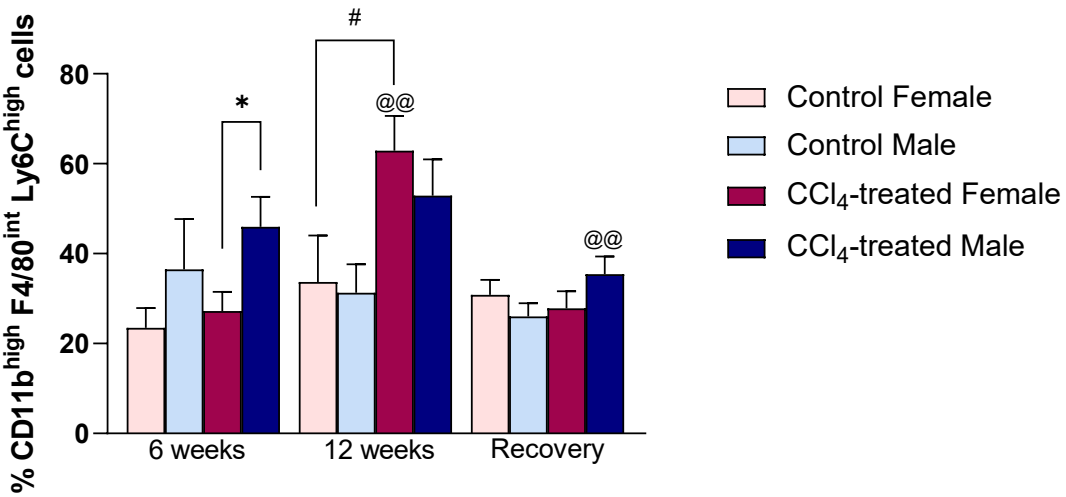

Figure 23 ***Quantification of MOMF Ly6C high of female mice (A) and male mice (B).*** *The histogram represents the percentage of CD11b^{high}, F4/80^{int} , Ly6C^{high} cells on mice at weeks 6, 12, and recovery. #p<0,05, ##p<0,01, ###p<0,001, ####p<0 vs. control mice of the same gender.*

3.4 Quantitative real time PCR

The effect of CCl_4 treatment in mice was assessed also by determining the difference in mRNA expression of some pro-inflammatory and fibrogenic elements by quantitative real-time PCR. The genes evaluated were Col1a1, Tgfβ, Ccl2, and Tnfα, Pdgf, Vegfa.

3.4.1 COL1A1

Col1a1 is the mRNA encoding for the major collagen produced by myofibroblasts In a healthy liver, normally, it is low expressed but the expression increases significantly during the fibrogenic process. [22]

The evaluation of Col1a1 was expressed as mRNA expression compared to the healthy female of 6 weeks. As shown in the *figure 25* there were no significant gender-related differences in Col1a1 mRNA expression among the different time points. However, there was a different trend between fibrotic females and fibrotic males in the mRNA expression of collagen.

After 6 weeks of CCl_4-treatment, fibrotic male mice showed higher levels of Col1a1 than fibrotic female mice. After 12 weeks the situation was inverted, fibrotic male mice had higher mRNA expression of collagen I than fibrotic female mice. Finally, at the end of the recovery period, Col1a1 mRNA levels decreased in fibrotic mice of both genders, with higher levels in fibrotic male mice than in fibrotic females. However, the gene expression of Col1a1 in fibrotic mice did not reach basal levels after the restorative phase. *(Figure 25)*

Even if we did not observe statistically significant differences in the mRNA expression of collagen type I, the trend we observed among the different time points was in line with the results we previously obtained with Masson's trichrome staining.

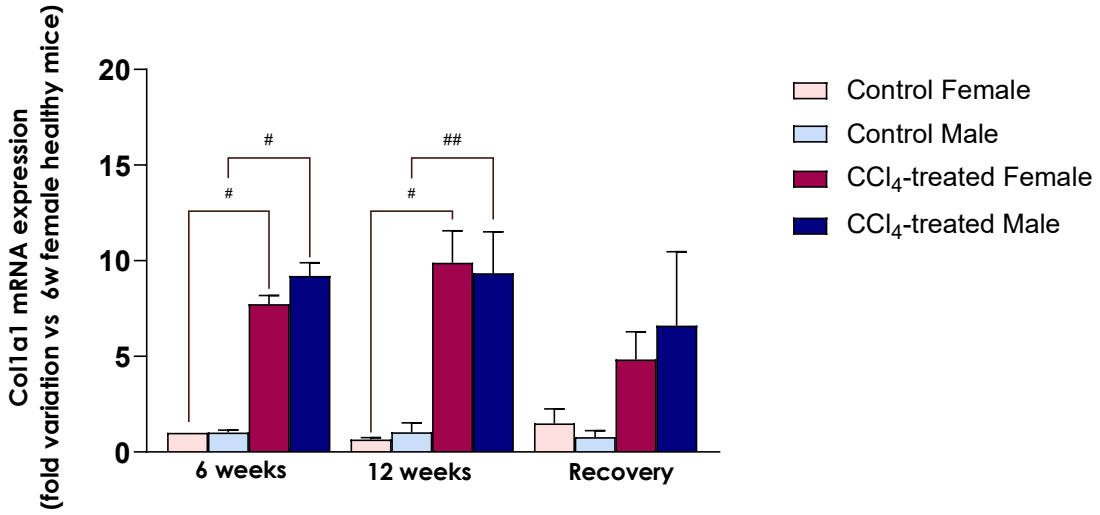

Figure 24. ***Real time-PCR for Col1a1 mRNA*** *of weeks 6, 12, and recovery. Results were normalized to those of mRNA encoding beta-actin and were calculated concerning control female mice of 6 weeks. Data are presented as mean ± SEM; $^{\#}p<0,05$ vs. control mice of the same gender.*

3.4.2 TGFβ

Tumour growth factor β1 (or TGFβ) is a profibrogenic cytokine. Since it has cytostatic and apoptotic effects on hepatocytes, it induces a massive hepatocyte cell death. Furthermore, TGFβ regulate the activation of Hepatic Stellate Cells, producing an increase of ECM deposition. [30]

TGFβ mRNA expression showed no significant difference between. However, after 6 weeks the TGFβ mRNA levels of fibrotic females were comparable to the ones observed in control mice. On the other hand, the mRNA expression of TGFβ was higher in fibrotic male mice than in their healthy counterpart and fibrotic females. After 12 weeks, the TGFβ mRNA levels slightly increased in fibrotic female mice and did not decrease after the recovery period. After 12 weeks, fibrotic male mice did not show variations in the gene expression of TGFβ but demonstrated a reduction to basal levels at the end of the restorative phase. *(Figure 26)*

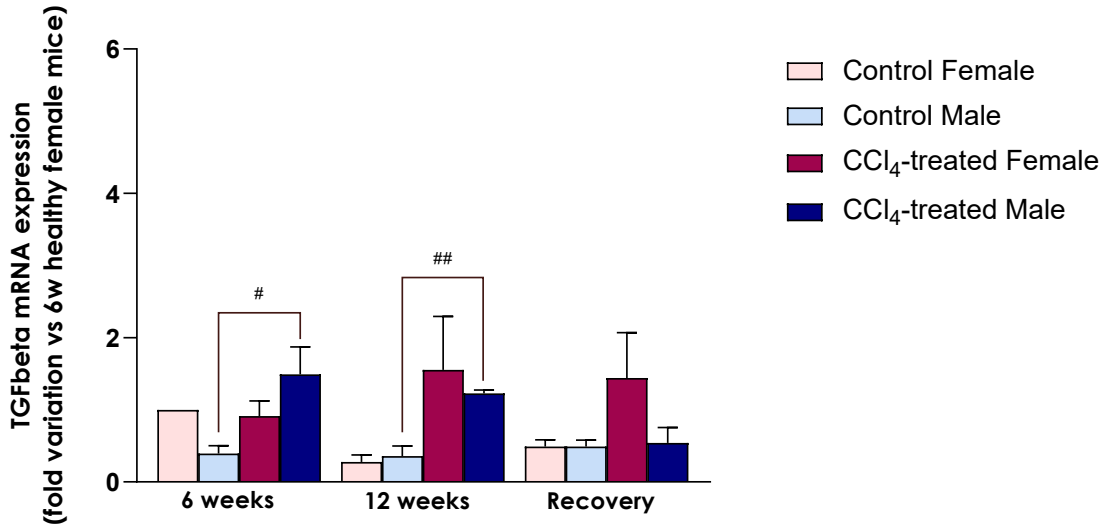

Figure 25 ***Real time-PCR for Tgfβ mRNA of weeks 6, 12, and recovery.*** *Results were normalized to those of mRNA encoding beta-actin and are calculated concerning control female mice of 6 weeks. Data are presented as mean ± SEM; $^{\#}p<0,05$ vs. control mice of the same gender.*

3.4.3 CCL2

Chemokine CCL2 (or Monocyte chemoattractant protein-1, MCP1) is secreted at high levels by Kupffer cells, injured hepatocytes and activated HSC. By the interaction with its receptors CCR2 on the surface of bone marrow-derived monocytes that differentiate into inflammatory macrophages inducing its accumulation in injured livers., expanding massively the quantity of local macrophage pool [31]

After 6 weeks, the mRNA levels of CCL2 increased in fibrotic mice of both genders with respect to control mice, with no particular sex dimorphism. After 12 weeks of CCl_4-treatment CCL2 mRNA levels massively increased in fibrotic female mice and the quantity of this chemokine was even higher than in fibrotic males. At the end of the recovery period, the gene expression of CCL2 rapidly decreased in fibrotic females, while did not in fibrotic male mice. However, the levels of this chemokine in fibrotic mice did not reach basal levels during liver regeneration. *(Figure 27)*

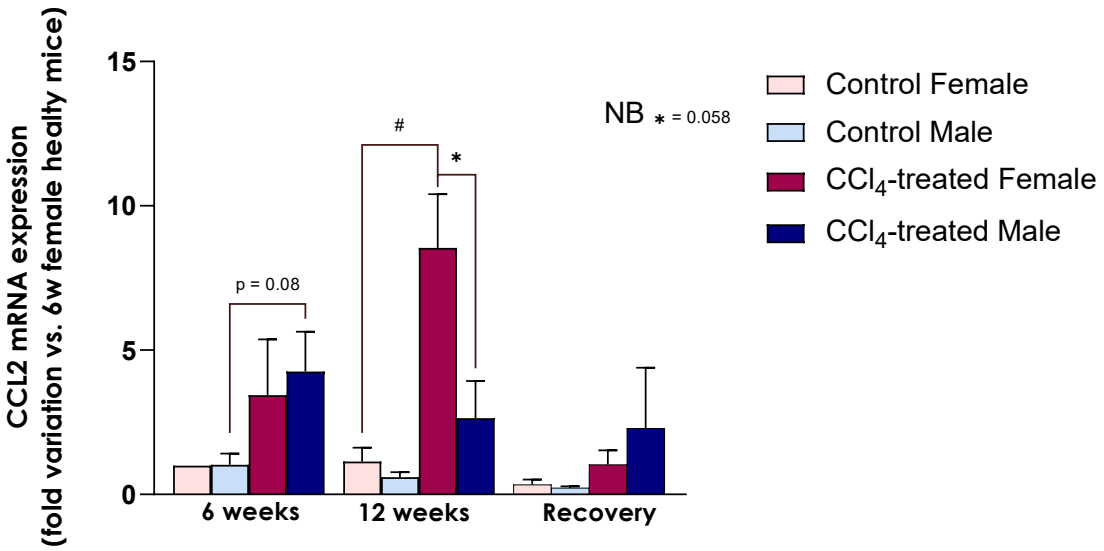

Figure 26 **Real time-PCR for Ccl2 mRNA of weeks 6, 12, and recovery**. Results were normalized to those of mRNA encoding beta-actin and are calculated concerning control female mice of 6 weeks. Data are presented as mean ± SEM; $^{\#}p<0,05$ vs. control mice of the same gender.

3.4.4 TNFα

Tumor necrosis factor-α (TNFα) is the key inflammatory cytokine involved in liver inflammation. It has a role in several processes and cells during the liver fibrosis. In HSC, it has a prosurvival effect and induce the expression of MMPs and relative inhibitors (TIMPs). Moreover, TNFα induce immunogenic and proinflammatory activity of dendritic cells, and in the end induce also an increased hepatocyte death rate. [32]

Tnfα mRNA PCR analysis showed an increased expression in fibrotic mice at 6 weeks with respect to controls, with no relevant sex differences. At 12 weeks, this cytokine produce a huge increase especially in male mice, while the female mice remain constant. After the recovery period, Tnfα returns to basal levels in males while in female remain constant. *(Figure 28)*

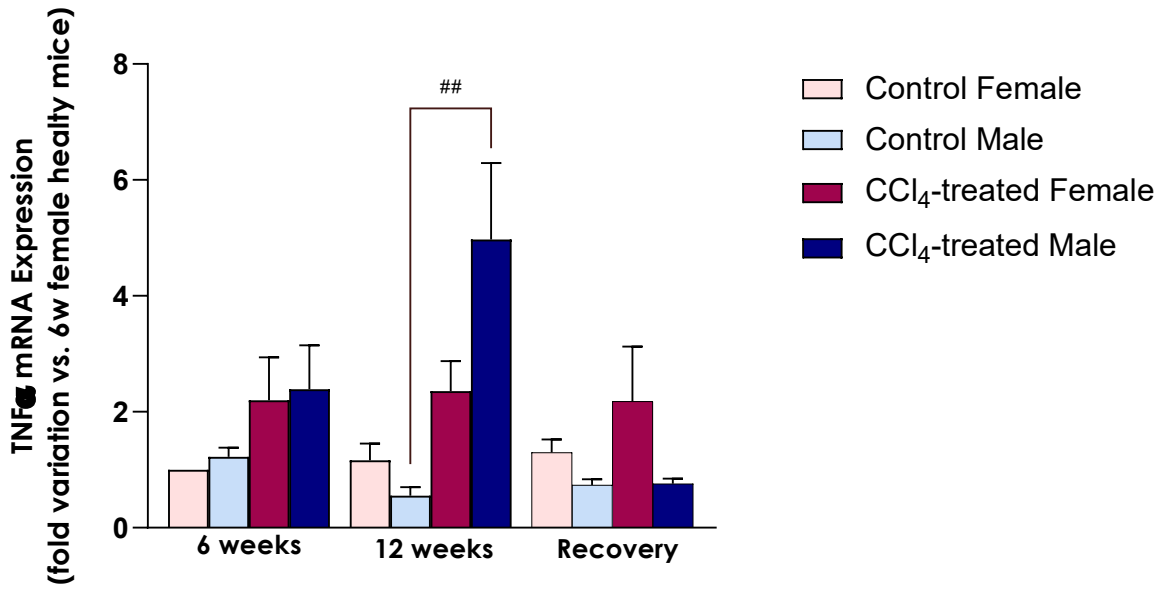

Figure 27 ***Real time-PCR for Tnfα mRNA of weeks 6, 12, and recovery.*** *Results were normalized to those of mRNA encoding beta-actin and are calculated concerning control female mice of 6 weeks. Data are presented as mean ± SEM; $^{\#}p<0,05$ vs. control mice of the same gender.*

3.4.5 PDGF

Platelet derived growth factor (PDGF) is the most potent factor involved in hepatic stellate cells proliferation, differentiation, and migration. After a liver injury occurs the expression increase producing an increase in chemotaxis and a decrease amount of Vitamin A stored in HSC, showing that is implicated in promotion of collagen I production and deposition. The A form show lower fluctuation than the others during the trans-differentiation of HSC into myofibroblasts. [33]

After 6 weeks, the mRNA levels of PDGFA increased in fibrotic mice of both genders with respect to control mice, with no particular sex dimorphism. After 12 weeks of CCl_4-treatment PDGFA mRNA levels massively increased in fibrotic male mice and the quantity of this cytokine was even higher than in fibrotic females. At the end of the recovery period, the gene expression of PDGFA decreased in both genders. However, the levels of PDGFA in fibrotic mice did not reach basal levels during liver regeneration. *(Figure 29)*

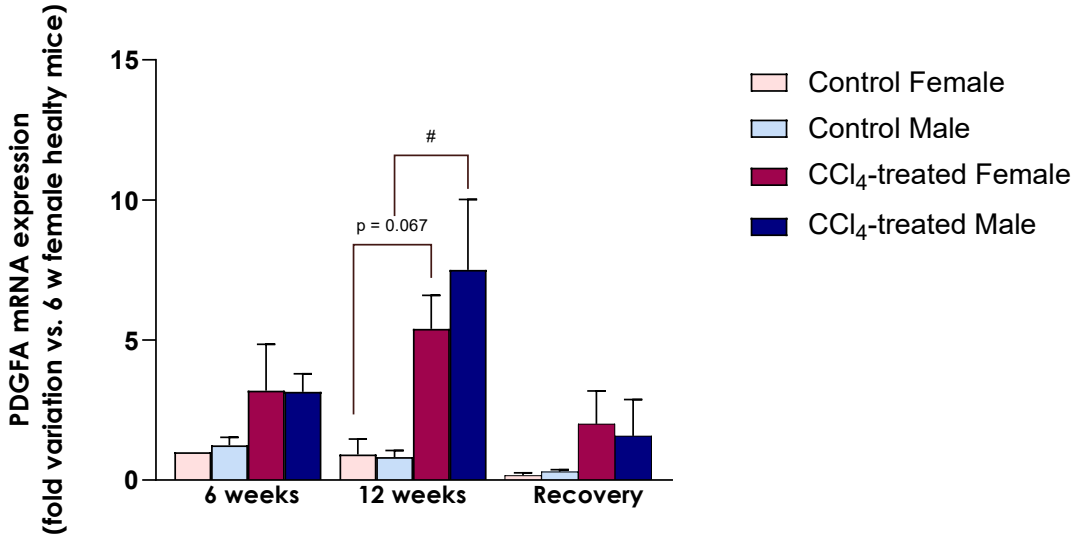

Figure 28 ***Real time-PCR for Pdgfa mRNA of weeks 6, 12, and recovery.*** *Results were normalized to those of mRNA encoding beta-actin and are calculated concerning control female mice of 6 weeks. Data are presented as mean ± SEM; $^{\#}p<0,05$ vs. control mice of the same gender.*

3.4.6 VEGFA

Vascular Endothelial Growth Factor A (or VEGFA) is a monocyte chemoattractant and a vascular permeability factor that revealed a dual effect in both fibrogenic and reparative processes. In fibogenesis it acts through promotion of inflammation, and the overexpression has direct effects on HSC increasing collagen deposition. Moreover, it shows a relevant effect also in the reparation process by VEGF- mediated ECM degradation due to upreguation of MMPs and downregulation of TIMPs in sinusoidal endothelial cells. [22]

At 6 weeks of treatment the mRNA expression of VEGFA show a huge increase in fibrotic mice than controls, especially in female. At 12 weeks, VEGF return to basal levels in both genders. After the recovery period, there is an increase of its expression in fibrotic mice compared to healthy ones, especially in female mice, although not significant. (*Figure 30*).

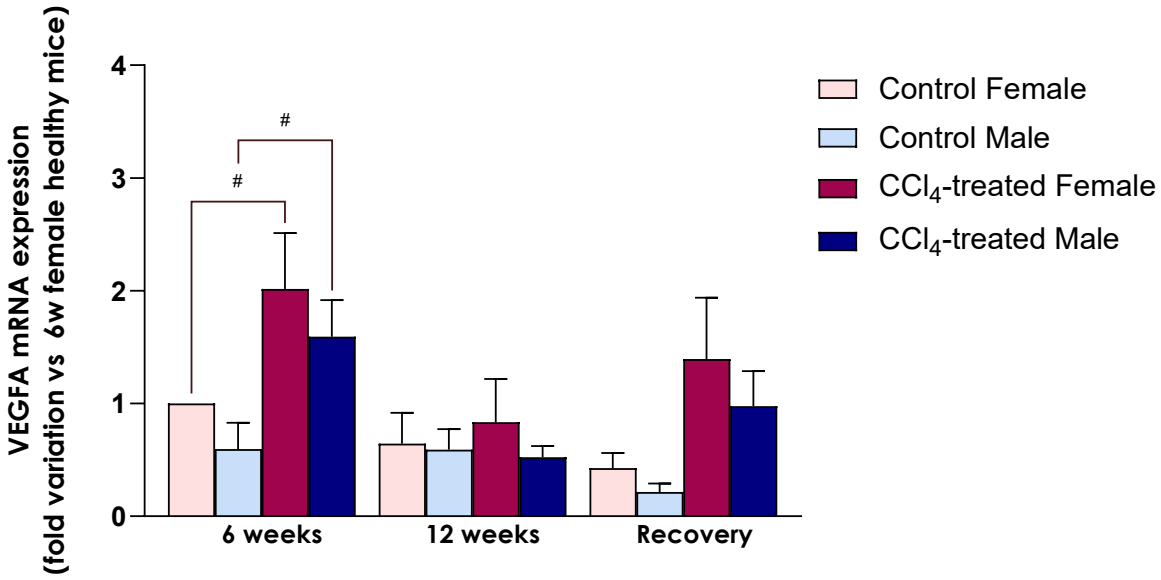

Figure 29 ***Real time-PCR for VEGFa mRNA of weeks 6, 12, and recovery.*** *Results were normalized to those of mRNA encoding beta-actin and are calculated concerning control female mice of 6 weeks. Data are presented as mean ± SEM; $^{\#}p<0,05$ vs. control mice of the same gender.*

DISCUSSION

Liver fibrosis represent an excessive wound-healing response to persistent hepatic injury. Clinical studies underline that there is a rise of prevalence of fibrosis, i.e. in US population there is an increase from 18% in 1988-1991 to 31% in 2011-2012, with a higher prevalence in men than in women. [34] Fibrotic scars are characterized by an excessive deposition of ECM due to dysregulation of the equilibrium between the production and degradation of the matrix. Liver fibrosis is a reversible process, but if the chronic source of injury persists it can degenerate into cirrhosis, an irreversible stage of liver scarring. In case of persistent damage, cirrhosis can result in hepatocellular carcinoma, organ failure and death. [20]

Hepatic Stellate Cells are the primary effector cells that drive liver fibrogenesis. They are activated by a pool of cytokines and chemokines including TGFβ, TNFα, and CCL2 released by Kupffer cells (KC) and damaged hepatocytes after a persistent liver injury. After their activation, HSCs transdifferentiate into myofibroblasts, secreting a large amount of ECM and pro-inflammatory cytokines. [35]

Kupffer cells recruit to the liver a subset of pro-fibrogenic Monocyte-derived macrophages, known as Ly6C^{high} macrophages. They infiltrate into the liver after being recruited by pro-inflammatory cytokines and promote damage. [8]

Kupffer cells, the resident liver macrophages, have a central role in regulating the production of MMP9. This endopeptidase has the role to degrade the ECM. During liver injury, the expression of MMPs is reduced, while the expression of their inhibitors TIMPs is increased. Changes in the expression of these enzymes produce a marked reduction in ECM degradation. [8]

An important feature of the liver is its ability to regenerate. In fact, after the removal of the source of injury, Profibrogenic Momφs switch the phenotype from Ly6C ^{high} to Ly6C ^{low}, also called restorative macrophages. They induce the the activated HSCs undergo apoptosis blocking the production of ECM. This produce also the re-establishing of equilibrium between TIMP1 and MMP9 with consequent increased degradation of ECM. [36]

There is also a marked sex dimorphism both in the progression and regression of liver fibrosis due to underline differences in a range of immune processes i.e. recruitment of infiltrated neutrophils and monocyte-derived macrophages. Furthermore, some studies showed a female heightened immune reactogenicity. This research aims to assess the

difference between the two genders in animal models, and the role of immune cells involved. [29]

In this work, we used male and female Balb/CJ mice treated with increasing doses of CCl_4 by intraperitoneal injections twice a week (from 0,17 µL/g to 0,72 µL/g). Male and female controls were injected with corn oil. Mice were treated with CCl_4 for 12 weeks followed by 8 weeks of washout period without treatment. They were sacrificed after 6 and 12 weeks of CCl4 treatment to assess hepatic damage and fibrosis progression, and after 8 weeks of washout period to assess liver regeneration.

The results obtained from the histological analysis underlined that all the CCl_4-treated animals exhibited hepatic fibrosis, while corn-oil treated showed a healthy liver. We observed different grades of liver fibrosis in the two genders and at three time points. From the quantification of fibrotic septa, after 6 weeks of treatment with CCl_4, the collagen areas were higher in treated mice than control mice, with a more severe increment in males compared to females. After 12 weeks of CCl_4 treatment, the degree of fibrosis became comparable between genders and after the recovery period, the regression occurred more efficiently in females than males. These observations underlined that males developed hepatic damage faster than females, and females showed a better regeneration of the parenchyma.

The quantification of alpha-SMA expression underline that treated male mice had higher activation of HSCs after 6 weeks of CCl_4 when compared to females. After 12 weeks occur a further increase leading to no difference between gender. During the recovery period occurs a gradual decrease of presence, especially in females. These results confirm the main role of HSCs in the development of liver fibrosis. Furthermore, these results follow the information obtained by Trichrome Stain that shows higher damage in males liver at early stage of fibrogenesis compared to females.

The MMP9 levels analyzed by Immunohistochemistry showed that after 6 weeks of CCl_4 treatment there was a lower expression in fibrotic mice, when compared to healthy mice. On the other hand, a huge increase of this enzyme occured during the recovery period, especially in treated females. These results based on their degrading activity, suggested a reduced degradation of ECM during the treatment, while the recovery of the activity after the washout period confirm the diminishing of damage seen with Trichrome Stain in this period.

The levels of tissue inhibitors of metalloproteinases (TIMPs) increased after 6 weeks of treatment in fibrotic mice than in healthy mice, showing sex dimorphism. After 12 weeks of CCl_4-treatment a further increase occurred in females, underlying sex-related differences. At the end, during liver regeneration, the levels of TIMP1 significantly decreased, especially in fibrotic females. These observations suggested a great inhibition of metalloproteases during the treatment and the reacquisition of their activity during the recovery period.

Significant differences were present in the neutrophils recruited in the liver. After 6 weeks of treatment there was a huge increase of these cells in fibrotic mice compared to healthy ones, especially in males. Since an excessive recruitment of neutrophils induces inflammation, this value is compatible to the higher damage underlined by Trichrome Stain after 6 weeks in males. At the end of the treatment and recovery period the levels of neutrophils returned to basal levels.

Other immune cells that might have a role in fibrogenesis are lymphocytes and NK cells. Chronic injury in liver produce infiltration of lymphocytes in the damaged regions. They can interact with ECM and contribute to the fibrogenic response by cell activation and differentiation. Our results showed a constant level of lymphocytes in fibrotic mice compared to the healthy ones during the treatment while there was an increased level during regeneration. These findings suggested a role of lymphocytes and NK in liver repair after the damage that was more efficient in females than males.

Some studies suggested that there is a decreased presence of KC during inflammation, due to the loss of essential cell-cell circuits and low plasticity, two essential features for KCs to adapt to the new microenvironment. We assessed that the reduction was evident at each timepoint in fibrotic mice from both genders, when compared to controls. Interestingly, after the recovery period, an increment of KC levels occurred, probably thanks to the reestablishment of a normal microenvironment.

The recruitment levels of pro-inflammatory macrophages $Ly6C^{high}$ $F4/80^{int}$ $CD11b^{high}$ showed a significant difference between fibrotic mice compared to healthy mice, confirming the critical role of these cells in fibrosis progression. The values obtained after 6 weeks was higher in treated males compared to females. As in other infiltrating immune

cells the percentage decreased after the end of the washout period, suggesting a switch of the phenotype to Ly6c^{low} as pro-restorative macrophages

Interestingly, the percentage of this population decreased after the washout period in fibrotic mice from both genders, corroborating the hypothesis that, when suspending the toxic insult, the liver can regenerate by reducing the inflammation induced by infiltrating immune cells.

In liver fibrosis, the composition of the Extracellular Matrix changed during the fibrotic process. During liver fibrosis occurred an increase in collagen types I, III, and IV. Moreover, several cytokines might directly stimulate the transcription of collagen type I in HSCs. For this reason, we evaluated mRNA expression of Col1a1. The results we obtained showed an upregulation of Col1a1 in CCl_4-treated mice during the CCl_4-treatment period, while after the washout period the mRNA levels of Col1a1 decreased in fibrotic mice from both genders, without reaching basal values.

Tumor necrosis factor alpha (Tnfα) is an important cytokine produced by a wide range of cells that induces proinflammatory activity like cellular proliferation, induction of other inflammatory mediators, and hepatocytes cell death. Our results showed a higher gene expression of Tnfα in fibrotic mice during the CCl_4-treatment period, when compared to healthy ones. After 12 weeks of treatment, a huge increase of Tnf alpha mRNA levels in male mice suggested a sex dimorphism. At the end of the recovery period, a decrement of the mRNA levels of this cytokine was noticed in fibrotic mice, especially in males, underlying gender-related differences. These results showed a reduction of inflammation after the washout period.

Transforming growth factor (TGF beta) is the major profibrogenic cytokine that drives HSC activation and induces ECM production. We observed a higher gene expression of TGF beta in males during the early stages of fibrosis development, while there was a decreasing after the washout period. While females show a gradual increase, reaching the pick at 12 weeks of treatment that remains stable also in the recovery period.

CCL2 is one of the most important chemokines, its expression is associated with the infiltration of monocytes that express the receptor CCL2R. It is secreted by Hepatocytes, Kupffer cells, and HSCs. This chemokine critically controls the accumulation of inflammatory monocyte-derived macrophages Ly6C+ in injured livers. Our results showed an initial increase of CCL2 mRNA levels in fibrotic mice concerning healthy mice, with no sex dimorphism. A massively increment in the gene expression of CCL2 was

observed in fibrotic female mice at the end of the treatment. During the recovery period, the gene expression of CCL2 rapidly decreased in fibrotic females, while did not in fibrotic male mice. This evidence suggested that in females occurred gradual inflammation that recovered during the washout period, while for males there was a permanent inflammation during the three-time points.

PDGFA is the most potent factor involved in hepatic stellate cell proliferation, differentiation, and migration. When liver injury occurs, the expression of PDGFA increases, producing an increase in chemotaxis and a decreased amount of Vitamin A stored in HSC. In this way, PDGFA is implicated in the promotion of collagen I production and deposition. The A form shows lower fluctuation than the others during the trans-differentiation of HSC into myofibroblasts. After 6 weeks, the mRNA levels of PDGFA increased in fibrotic mice of both genders concerning control mice, with no particular sex dimorphism. After 12 weeks of CCl_4-treatment PDGFA mRNA levels massively increased in fibrotic male mice and the quantity of this cytokine was even higher than in fibrotic females. At the end of the recovery period, the gene expression of PDGFA rapidly decreased in both genders. However, the levels of PDGFA in fibrotic mice did not reach basal levels during liver regeneration.

It has been demonstrated that VEGFA plays a critical role in fibrogenesis. This vascular permeability factor can regulate the recruitment and infiltration of monocytes. Moreover, it plays a fibrogenic effect through multiple mechanisms, including the promotion of inflammation, the release of fibrosis-enhancing molecules, and direct effects on HSCs. However, VEGFA also induces angiogenesis and contributes to wound healing and tissue repair. In the early stage of treatment, the mRNA expression of VEGFA showed a big increase in female fibrotic mice than in controls. After 12 weeks, VEGF returns to basal levels in both genders, while after the recovery period, there was an increase of VEGFA expression in fibrotic mice compared to healthy ones, especially in female mice. These results suggested a great recruitment during the 6 weeks of treatment, while an increase during the recovery period contributed to angiogenesis and tissue repair.

CONCLUSIONS

In conclusion, we obtained a murine model of progressive liver fibrosis by administering increasing doses of CCl_4 for 12 weeks. We were also able to study liver regeneration after a washout period of 8 weeks, after the CCl_4 treatment period. This model was useful to assess gender differences in fibrogenesis and liver repair.

Males showed higher hepatic damage in the first stage of toxic insult, since they presented higher HSCs activation, and a higher expression of metalloproteinase inhibitors (TIMPs), pro-inflammatory cytokines and chemokines, and increased infiltration of recruited immune cells. Females showed a more gradual damage, as suggested by the levels of activated HSCs, the expression of TIMPs, chemokines, and cytokines after 12 weeks of CCl_4. After the recovery period, females showed a higher capacity for liver regeneration.

Moreover, future investigations are needed to assess the translational value of our results, and to better clarify the cellular mechanisms and immune responses involved in liver injury and regeneration.

BIBLIOGRAPHY

1. Sherif R. Z. Abdel-Misih, Mark Bloomston. Liver anatomy. 643–53 (2010).

2. Ozougwu, Jevas C. Physiology of the liver. *Int. J. Res. Pharm. Biosci.* **4**, 13–24 (2017).

3. Eszter Nemeth, Alan W. Baird, Cliona O'Farrelly. microanatomy of the liver immune system. *semin immunopathol* 333–343 (2009) doi:10.1007/s00281-009-0173-4.

4. Lena Sibulesky. normal liver anatomy. *Clinical Liver Disease* s1–s3 (2013) doi:10.1002/cld.124.

5. Amit Panwar, Prativa Das and Lay Poh Tan. 3D Hepatic Organoid-Based Advancements in LIVER Tissue Engineering. *Bioengineering* **8**, (2021).

6. Martin, Meek, and Willebtry. *Veterinary Histology*. (LibreTexts).

7. Liver. https://anatomy.co.uk/liver/.

8. George Kolios, Vassilis Valatas, Elias Kouroumalis. Role of Kupffer cells in the pathogenesis of liver disease. *World J. Gastroeneterology* **12**, 7413–7420 (2006).

9. Min Feng1*, Jie Ding1*, Min Wang2, Jie Zhang1,2, Xinhua Zhu1 and Wenxian Guan1. kupffer-derived matrix metalloproteinase-9 contributes to liver fibrosis resolution. *Int. J. Biol. Sci.* **14**, 1033–1040 (2018).

10. Cheng D, Chai J, Wang H, Fu L, Peng S, Ni X. Hepatic macrophages: Key players in the development and progression of liver fibrosis. *Liver Int* **41**, 2279–2294 (2021).

11. Mossanen JC, Tacke F. Role of lymphocytes in liver cancer. Oncoimmunology. *Oncoimmunology* **2**, (2013).

12. Kubes P, Jenne C. Immune Responses in the Liver. *Annu Rev Immunol* **36**, 247–277 (2018).

13. Yanan Wang, Cai Zhang. The Roles of Liver-Resident Lymphocytes in Liver Diseases. *Front Immunol* (2019).

14. Liu P, Chen L, Zhang H. Natural Killer Cells in Liver Disease and Hepatocellular Carcinoma and the NK Cell-Based Immunotherapy. *J. Immunol.* (2018) doi:doi: 10.1155/2018/1206737.

15. Tang J, Yan Z, Feng Q, Yu L, Wang H. The Roles of Neutrophils in the Pathogenesis of Liver Diseases. *Front Immunol* **12**, (2021).

16. Kolaczkowska E, Kubes P. Neutrophil recruitment and function in health and inflammation. *Nat Rev Immunol* **13**, 159–175 (2013).

17. Cho Y, Szabo G. Two Faces of Neutrophils in Liver Disease Development and Progression. *Hepatology* **74**, 503–512 (2021).

18. Yang W, Tao Y, Wu Y, Zhao X, Ye W, Zhao D, Fu L, Tian C, Yang J, He F, Tang L. Neutrophils promote the development of reparative macrophages mediated by ROS to orchestrate liver repair. *Nat Commun* **10**, 1076 (2019).

19. Zimmermann HW, Bruns T, Weston CJ, Curbishley SM, Liaskou E, Li KK, Resheq YJ, Badenhorst PW, Adams DH. Bidirectional transendothelial migration of monocytes across hepatic sinusoidal endothelium shapes monocyte differentiation and regulates the balance between immunity and tolerance in liver. *Hepatology* **63**, 233–246 (2015).

20. Tan Z, Sun H, Xue T, Gan C, Liu H, Xie Y, Yao Y, Ye T. Liver Fibrosis: Therapeutic Targets and Advances in Drug Therapy. *Front Cell Dev Biol* **9**, (2021).

21. Zhang CY, Yuan WG, He P, Lei JH, Wang CX. Liver fibrosis and hepatic stellate cells: Etiology, pathological hallmarks and therapeutic targets. *World J Gastroenterol* **22**, 10512–10522 (2016).

22. Natascha Roehlen, Emilie Crouchet and Thomas F. Baumert. Liver Fibrosis: Mechanistic Concepts and Therapeutic Perspectives. *MDPI - Cells* **9**, (2020).

23. Patrizia Burra, Debora Bizzaro, Anna Gonta, Sarah Shalaby, Martina Gambato, Maria Cristina Morelli, Silvia Trapani, Annarosa Floreani, Fabio Marra, Maurizia Rossana Brunetto, Gloria Taliani, Erica Villa. Clinical impact of sexual dimorphism in non-alcoholic fatty liver disease (NAFLD) and non-acoholic steatohepatitis (NASH). *Liver Int. J.* **41**, 1713–1733 (2021).

24. Claire E. McQuitty, Roger Williams, Shilpa Chokshi, and Luca Urbani. Immunomodulatory Role of the Extracellular Matrix Within the Liver Disease Microenvironment. *Front. Immunol.* **11**, (2020).

25. Adnan Naim, Qiuwei Pan, Mirza S. Baig. Matrix Metalloproteinases (MMPs) in Liver Diseases. *J. Clin. Exp. Hepatol.* **7**, 367–372 (2017).

26. Fangming Yang, Heng Li, Yanmin Li, Yaokun Hao, Chenxiao Wang, Pan Jia, Xinju Chen, Suping Ma, Zhun Xiao. Crosstalk between hepatic stellate cells and surrounding cells in hepatic fibrosis. *Int. Immunopharmacol.* **99**, (2021).

27. Alessandra Caligiuri, Alessandra Gentilini , Mirella Pastore, Stefano Gitto and Fabio Marra. Cellular and Molecular Mechanisms Underlying Liver Fibrosis Regression. *MDPI - Cells* **10**, (2021).

28. Philippe Lefebvre and Bart Staels. Hepatic sexual dimorphism - implications for non-alcoholic fatty liver disease. *Endocrinology* **17**, 662–670 (2021).

29. Sebastien Jaillon, Kevin Berthenet, Cecilia Garlanda. Sexual Dimorphism in Innate Immunity. *Clin. Rev Allerg Immunol* **56**, 308–321 (2019).

30. Isabel Fabregat, Joaquim Moreno-Caceres, Aranzazu Sanchez, Steven Doole, Bedair Dewidar, Gianluigi Giannelli and Peter ten Dijke. TGF-b signalling and liver disease. *Febs J.* **283**, 2219–2232 (2016).

31. Josef Ehling, Matthias Bartnech, Xiao Wei, Felix Gremse, Viktor Fech, Diana Möckel, Christer Baeck, Kanishka Hittatiya, Dirk Eulberg, Tom Luedde, Fabian Kiessling, Christian Trautwein, Twan Lammers, and Frank Tacke. CCL2-dependent infiltrating macrophages promote angiogenesis in progressive liver fibrosis. *Gut* **63**, 1960–1971 (2014).

32. Fabio Marra and Frank Tacke. Roles of Chemokines in Liver Disease. *Gastroenterology* **147**, 577–594 (2014).

33. Erawan Borkham-Kamphorst, Ralf Weiskirchen. The PDGF system and its antagonists in liver fibrosis. *Cytokines Growth Factor Rev.* **28**, 53–61 (2016).

34. Shaheen M, Schrode KM, Pan D, Kermah D, Puri V, Zarrinpar A, Elisha D, Najjar SM, Friedman TC. Sex-Specific Differences in the Association Between Race/Ethnicity and NAFLD Among US Population. *Front Med* **8**, (2021).

35. Zhang M, Serna-Salas S, Damba T, Borghesan M, Demaria M, Moshage H. Hepatic stellate cell senescence in liver fibrosis: Characteristics, mechanisms and perspectives. *Mech Ageing Dev* **199**, (2021).

36. Tatiana Kisseleva and David Brenner. Molecular and cellular mechanisms of liver fibrosis and its regression. *Gastroenterol. Hepatol.* **18**, 151–162 (2021).